REPORT DOCUMENTATION PAGE

Form Approved OMB NO. 0704-0188

The public reporting burden for this collection of information is estimated to average 1 hour per response, including the time for reviewing instructions, searching existing data sources, gathering and maintaining the data needed, and completing and reviewing the collection of information. Send comments regarding this burden estimate or any other aspect of this collection of information, including suggesstions for reducing this burden, to Washington Headquarters Services, Directorate for Information Operations and Reports, 1215 Jefferson Davis Highway, Suite 1204, Arlington VA, 22202-4302. Respondents should be aware that notwithstanding any other provision of law, no person shall be subject to any oenalty for failing to comply with a collection of information if it does not display a currently valid OMB control number.
PLEASE DO NOT RETURN YOUR FORM TO THE ABOVE ADDRESS.

1. REPORT DATE (DD-MM-YYYY)	2. REPORT TYPE	3. DATES COVERED (From - To)
08-05-2012	Final Report	1-Jun-2007 - 31-Jul-2012

4. TITLE AND SUBTITLE
Monolithic Micromachined Quartz Resonator based Infrared Focal Plane Arrays
FINAL REPORT

5a. CONTRACT NUMBER: W911NF-07-1-0327

5b. GRANT NUMBER:

5c. PROGRAM ELEMENT NUMBER: 611102

5d. PROJECT NUMBER:

5e. TASK NUMBER:

5f. WORK UNIT NUMBER:

6. AUTHORS
Srinivas Tadigadapa

7. PERFORMING ORGANIZATION NAMES AND ADDRESSES
Pennsylvania State University
Office of Sponsored Programs
The Pennsylvania State University
University Park, PA 16802 -7000

8. PERFORMING ORGANIZATION REPORT NUMBER

9. SPONSORING/MONITORING AGENCY NAME(S) AND ADDRESS(ES)
U.S. Army Research Office
P.O. Box 12211
Research Triangle Park, NC 27709-2211

10. SPONSOR/MONITOR'S ACRONYM(S)
ARO

11. SPONSOR/MONITOR'S REPORT NUMBER(S)
52257-EL.17

12. DISTRIBUTION AVAILABILITY STATEMENT
Approved for Public Release; Distribution Unlimited

13. SUPPLEMENTARY NOTES
The views, opinions and/or findings contained in this report are those of the author(s) and should not contrued as an official Department of the Army position, policy or decision, unless so designated by other documentation.

14. ABSTRACT
This report summarizes the design, fabrication, and characterization of thermal infrared (IR) imaging arrays operating at room temperature which are based on Y -cut-quartz bulk acoustic wave resonators. A novel method of tracking the resonance frequency based upon the measurement of impedance is presented. High-frequency (240-MHz) micromachined resonators from Y -cut-quartz crystal cuts were fabricated using heterogeneous integration techniques on a silicon wafer. A temperature sensitivity of 22.16 kHz/?C was experimentally

15. SUBJECT TERMS
Project Final Report

16. SECURITY CLASSIFICATION OF: a. REPORT	b. ABSTRACT	c. THIS PAGE	17. LIMITATION OF ABSTRACT	15. NUMBER OF PAGES	19a. NAME OF RESPONSIBLE PERSON
UU	UU	UU	UU		Srinivas Tadigadapa
					19b. TELEPHONE NUMBER: 814-865-2730

Standard Form 298 (Rev 8/98)
Prescribed by ANSI Std. Z39.18

Report Title

Monolithic Micromachined Quartz Resonator based Infrared Focal Plane Arrays
FINAL REPORT

ABSTRACT

This report summarizes the design, fabrication, and characterization of thermal infrared (IR) imaging arrays operating at room temperature which are based on Y -cut-quartz bulk acoustic wave resonators. A novel method of tracking the resonance frequency based upon the measurement of impedance is presented. High-frequency (240-MHz) micromachined resonators from Y -cut-quartz crystal cuts were fabricated using heterogeneous integration techniques on a silicon wafer. A temperature sensitivity of 22.16 kHz/?C was experimentally measured.IR measurements on the resonator pixel resulted in a noise equivalent power of 3.90 nW/Hz^1/2, a detectivity D? of 1 × 10^5 cmHz^1/2/W, and a noise equivalent temperature difference of 4 mK in the 8 -14 ?m wavelength range. The thermal frequency response of the resonator was determined to be faster than 33 Hz, demonstrating its applicability in video-rate uncooled IR imaging. This work represents the first comprehensive thermal characterization of micromachined Y -cut-quartz resonators and their IR sensing response. In addition the report also summarizes the work done on viscoelastic measurements performed using micromachined quartz resonators and quartz etching work undertaken as part of this work.

Enter List of papers submitted or published that acknowledge ARO support from the start of the project to the date of this printing. List the papers, including journal references, in the following categories:

(a) Papers published in peer-reviewed journals (N/A for none)

Received		Paper
2012/05/08 1!	7	Ping Kao, Srinivas Tadigadapa. Micromachined quartz resonator based infrared detector array, Sensors and Actuators A: Physical, (02 2009): 0. doi: 10.1016/j.sna.2008.11.013
2012/05/08 1!	6	Ping Kao, David Allara, Srinivas Tadigadapa. Fabrication and performance characteristics of high-frequency micromachined bulk acoustic wave quartz resonator arrays, measurement science and technology, (12 2009): 0. doi: 10.1088/0957-0233/20/12/124007
2012/05/08 1!	5	S Tadigadapa, K Mateti. Piezoelectric MEMS sensors: state-of-the-art and perspectives, measurement science and technology, (09 2009): 0. doi: 10.1088/0957-0233/20/9/092001
2012/05/08 1!	4	Marcelo B. Pisani, Kailiang Ren, Ping Kao, Srinivas Tadigadapa. Application of Micromachined <formula formulatype="inline"><tex Notation="TeX">Y</tex></formula> -Cut-Quartz Bulk Acoustic Wave Resonator for Infrared Sensing, Journal of Microelectromechanical Systems, (02 2011): 0. doi: 10.1109/JMEMS.2010.2100030
2012/05/08 1!	3	Ping Kao, David L. Allara, Srinivas Tadigadapa. Study of Adsorption of Globular Proteins on Hydrophobic Surfaces, IEEE Sensors Journal, (11 2011): 0. doi: 10.1109/JSEN.2011.2157819
2012/05/08 1!	2	Kailiang Ren, Ping Kao, Marcelo B. Pisani, Srinivas Tadigadapa. Monitoring biochemical reactions using Y-cut quartz thermal sensors, The Analyst, (06 2011): 0. doi: 10.1039/c1an15153c
2012/05/08 1!	1	Ping Kao, Purnendu Parhi, Anandi Krishnan, Hyeran Noh, Waseem Haider, Srinivas Tadigadapa, David L. Allara, Erwin A. Vogler. Volumetric interpretation of protein adsorption: Interfacial packing of protein adsorbed to hydrophobic surfaces from surface-saturating solution concentrations, Biomaterials, (2 2011): 0. doi: 10.1016/j.biomaterials.2010.09.075

TOTAL: 7

Number of Papers published in peer-reviewed journals:

(b) Papers published in non-peer-reviewed journals (N/A for none)

Received	Paper

TOTAL:

Number of Papers published in non peer-reviewed journals:

(c) Presentations

Number of Presentations: 0.00

Non Peer-Reviewed Conference Proceeding publications (other than abstracts):

Received	Paper

TOTAL:

Number of Non Peer-Reviewed Conference Proceeding publications (other than abstracts):

Peer-Reviewed Conference Proceeding publications (other than abstracts):

Received		Paper
2012/05/08 2(	14	Ping Kao, Matthew P Chang, David Allara, Srinivas Tadigadapa. Investigation of spontaneously adsorbed globular protein films using high-frequency bulk acoustic wave resonators, 2010 Ninth IEEE Sensors Conference (SENSORS 2010). 2010/11/01 00:00:00, Kona, HI. : ,
2012/05/08 2(	15	D. Allara, S. Tadigadapa, P. Kao. Label free piezoelectric DNA sensor array by selective immobilization via electrochemical method, 2011 IEEE 24th International Conference on Micro Electro Mechanical Systems (MEMS). 2011/01/23 00:00:00, Cancun, Mexico. : ,
2012/05/08 2(	16	M.B. Pisani, P. Kao, S. Tadigadapa. Bulk acoustic wave resonators for infrared detection applications, TRANSDUCERS 2009 - 2009 International Solid-State Sensors, Actuators and Microsystems Conference. 2009/06/21 00:00:00, Denver, CO, USA. : ,
2012/05/08 2(	12	Son Vu Hoang Lai, Ping Kao, Srinivas Tadigadapa. Thermal biosensors from micromachined bulk acoustic wave resonators, Eurosensors XXV Conference. 2011/09/04 00:00:00, . : ,
2012/05/08 2(	11	Hwall Min, David Allara, Srinivas Tadigadapa. Investigation of the Viscoelastic Properties of Liquids Trapped in Nanoporous Cavities using Micromachined Acoustic Transducers, Eurosensors XXV Conference. 2011/09/04 00:00:00, . : ,
2012/05/08 2(	10	Nichole Sullivan, Hwall Min, David Allara, Srinivas Tadigadapa. Nanoporous Gold: A High Sensitivity and Specificity Biosensing Substrate, Eurosensors XXV. 2011/09/04 00:00:00, . : ,
2012/05/08 2(	9	Marcelo B. Pisani, Kailiang Ren, Ping Kao, Srinivas Tadigadapa. Room temperature infrared imaging array fabricated using heterogeneous integration methods, Eurosensors XXIV Conference. 2010/09/05 00:00:00, . : ,
2012/05/08 2(	13	Ping Kao, Matthew P. Chang, David Allara, Srinivas Tadigadapa. Systematic studies on globular proteins using micromachined high frequency bulk acoustic wave resonators, Eurosensor XXIV Conference. 2010/09/05 00:00:00, . : ,
2012/05/08 1!	8	Kailiang Ren, Marcelo Pisani, Ping Kao, and Srinivas Tadigadapa. Micromachined Quartz Resonator based High Performance Thermal Sensors, IEEE Sensors Conference. 2010/11/01 00:00:00, . : ,

TOTAL: **9**

Number of Peer-Reviewed Conference Proceeding publications (other than abstracts):

(d) Manuscripts

Received Paper

TOTAL:

Number of Manuscripts:

Books

Received Paper

TOTAL:

Patents Submitted

Fabrication Method and Detection Enhancement Strategy for Ultra-Sensitive Temperature Detection Using Resonant Devices

Patents Awarded

Awards

Presented Paper selected one of the Best Papers presented at IEEE SENSORS 2010 in Hawaii and published as a paper in a Special Issue of IEEE Sensors Journal.

Graduate Students

NAME	PERCENT_SUPPORTED	Discipline
Ping Kao	0.10	
FTE Equivalent:	**0.10**	
Total Number:	**1**	

Names of Post Doctorates

NAME	PERCENT_SUPPORTED
Marcelo Pisani	1.00
FTE Equivalent:	**1.00**
Total Number:	**1**

Names of Faculty Supported

NAME	PERCENT_SUPPORTED	National Academy Member
Srinivas Tadigadapa	0.10	
FTE Equivalent:	**0.10**	
Total Number:	**1**	

Names of Under Graduate students supported

NAME	PERCENT_SUPPORTED	Discipline
Matthew Chang	0.05	Electrical Engineering
FTE Equivalent:	**0.05**	
Total Number:	**1**	

Student Metrics

This section only applies to graduating undergraduates supported by this agreement in this reporting period

The number of undergraduates funded by this agreement who graduated during this period:	1.00
The number of undergraduates funded by this agreement who graduated during this period with a degree in science, mathematics, engineering, or technology fields:......	1.00
The number of undergraduates funded by your agreement who graduated during this period and will continue to pursue a graduate or Ph.D. degree in science, mathematics, engineering, or technology fields:......	1.00
Number of graduating undergraduates who achieved a 3.5 GPA to 4.0 (4.0 max scale):	1.00
Number of graduating undergraduates funded by a DoD funded Center of Excellence grant for Education, Research and Engineering:	0.00
The number of undergraduates funded by your agreement who graduated during this period and intend to work for the Department of Defense	0.00
The number of undergraduates funded by your agreement who graduated during this period and will receive scholarships or fellowships for further studies in science, mathematics, engineering or technology fields:	1.00

Names of Personnel receiving masters degrees

NAME	
Total Number:	

Names of personnel receiving PHDs

NAME	
Ping Kao	
Total Number:	**1**

Names of other research staff

NAME	PERCENT_SUPPORTED
FTE Equivalent:	
Total Number:	

Sub Contractors (DD882)

Inventions (DD882)

5 **Fabrication Method and Detection Enhancement Strategy for Ultra-Sensitive Temperature Detection Using Resonant Devices**

Patent Filed in US? (5d-1) Y

Patent Filed in Foreign Countries? (5d-2) N

Was the assignment forwarded to the contracting officer? (5e) N

Foreign Countries of application (5g-2):

5a: Marcelo Pisani

5f-1a: The Pennsylvania State University

5f-c: 121 Electrical Engineering East Building

Uni versity Park PA 16802

5a: Srinivas Tadigadapa

5f-1a: The Pennsylvania State University

5f-c: 121 Electrical Engineering East Building

University Park PA 16802

Scientific Progress

Please see the attached Presentation File

Technology Transfer

PENNSTATE MEMS

Project Title: Monolithic Micromachined Quartz Resonator based Infrared Focal Plane Arrays

Project PI: Srinivas Tadigadapa

Department of Electrical Engineering

N-237 Millennium Science Center

Pennsylvania State University, University Park, PA 16802

Tel: 814 865 2730, Fax. 814 865 7065, e-mail: sat10@psu.edu

FINAL REPORT

Grant # W911NF-07-1-0327

Project Start Date: June 2007

Period of Reporting: August 2010 – April 2012

Program Manager: Dr. William Clark, Army Research Office

PENNSTATE MEMS

Main Goals of the Proposed Work

- In this proposal we aim to demonstrate IR staring arrays based on quartz crystal oscillators with a pitch of ~50 μm, NEDT of ~10 mK and a response time of ~10 ms eventually allowing for 100 frames/s video rate in the 8-14 μm IR wavelength range.
- A $25,000 addition to the proposal was added in November 2011 to explore high speed etching of glass using nitrogen trifluoride based gas.

Personnel Working on the Project

- Dr. Srinivas Tadigadapa, Professor, Penn State University (Principal Investigator)
- Dr. Marcelo Pisani, Post Doctoral Research Associate (Project Technical Leader)
- Dr. Ping Kao (Graduated with Ph.D. partially supported by this grant)
- Mr. Mathew Chang, BS Student (Data Acquisition Program Development)

Summary of Achievements

PENNSTATE MEMS

- The first prototypes of integrated micromachined IR detectors consisting of 200 μm diameter QCM resonators, 241 MHz (6.9 μm) thick 5 x 5 resonator arrays from Y-cut Quartz have been successfully fabricated. These are the thinnest Y-cut resonators fabricated to date.
- Established process flow to fabricate arrays of small QCM devices.
- A novel measurement method for the real-time tracking of the resonance frequency based on impedance measurement around the resonance frequency has been established.
- A patent disclosure was filed on the findings and methods of this work.
- Nitrogen trifluoride based glass etching process was started as part of this project and is still in progress.
- One student obtained his Ph.D. partially supported by this project and one post-doctoral research associate was trained on the project.

Report Overview

- The report is divided into the following main sections:
  - IR Detectors design, fabrication, and performance
  - Use of miniaturized quartz resonators for viscoelastic measurement applications (additional work done as part of this project)
  - Nitrogen trifluoride based etching of glass and quartz

SUMMARY OF QUARTZ RESONATOR BASED ROOM TEMPERATURE INFRARED IMAGING ARRAY

Thermal IR Sensing

- Thermal infrared detectors are broadband detectors and can be operated at room temperature without cooling.
- They have lower detectivity and slower response time in comparison to cooled semiconductor photonic detectors.
- Micromachined thermal detectors owing to their small thermal mass and good thermal isolation demonstrate much improved performance.
- These detectors can be designed to operate near the room temperature thermodynamic noise limit arising from the thermal conductance fluctuation between the sensing element and the supporting substrate.

Thermal Infrared Detectors: State of the Art

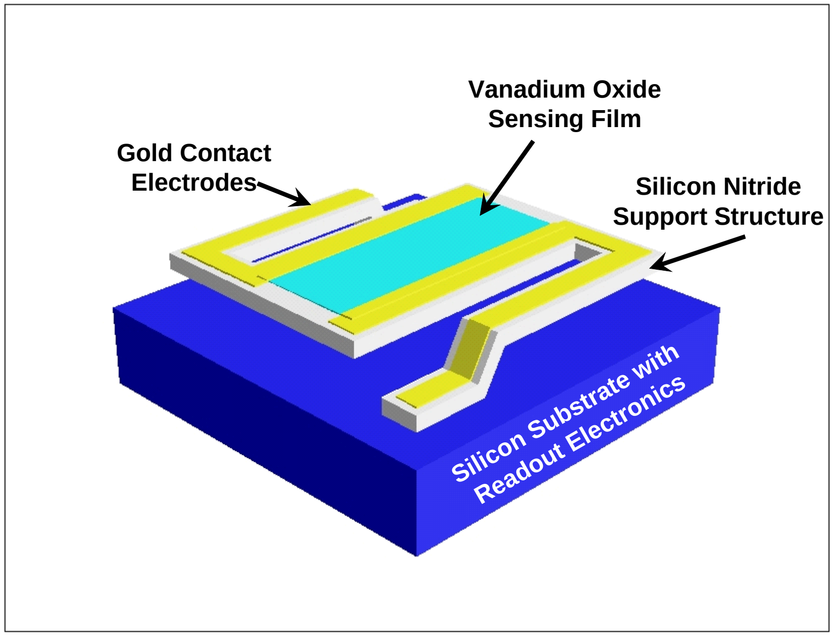

Vanadium Oxide based IR Detector configuration introduced by Honeywell in late 1990's & Perfected in 2000's.

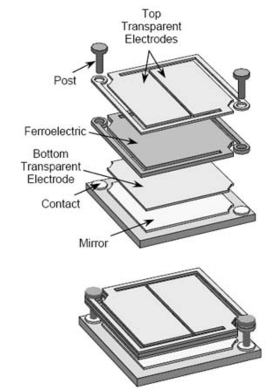

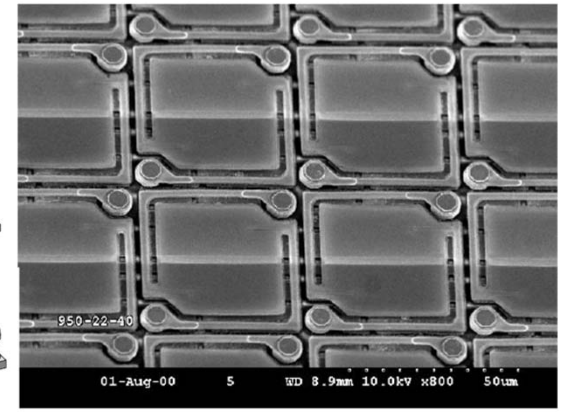

Lanthanum-doped lead zirconate titanate based focal plane array – developed by TI.

Wood R A, Proc. SPIE 2020 322–329, **1993**

Hanson C M, Beratan H R, and Belcher J F, Proc. SPIE 4288 298–303, **2001**

Quartz IR Detector: Goals

- Y-cut quartz is a sensitive temperature sensor capable of temperature resolution in μK.
- Develop micromachining process compatible for the production of 10 μm thick quartz resonators with minimal damping characteristics.
- This work demonstrates IR staring arrays based on quartz crystal oscillators:
  - Pitch of ~500 μm (Oscillator size 200 μm)
  - NEDT of <10 mK
  - Response time of ~10 ms allowing for 100 frames/s video rate in the 8-14 μm IR wavelength range.
- Develop thermal models to optimize the performance of the devices.

Conceptual Drawing of the Resonator

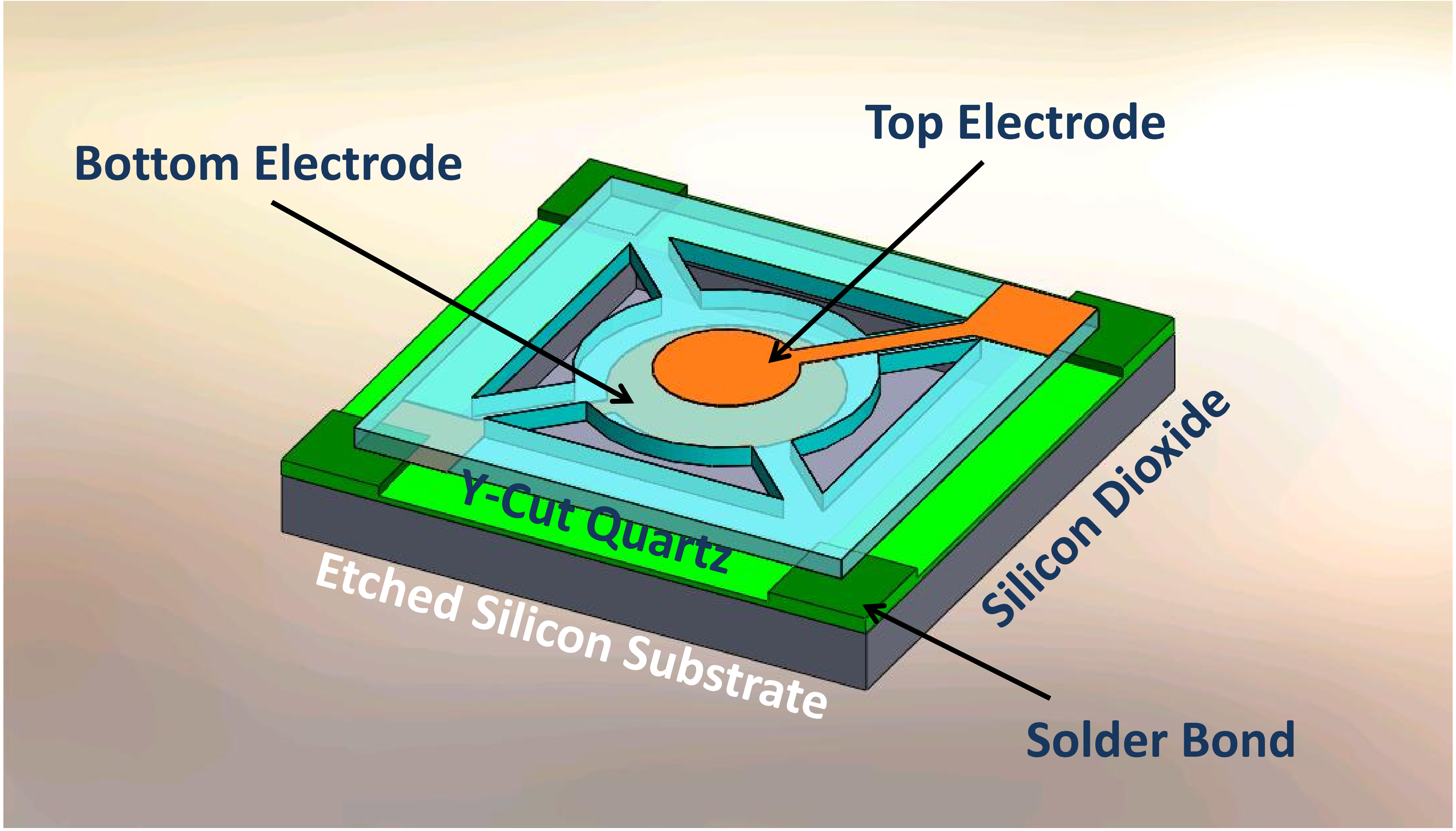

Device Design and Mask Layout

Overview of the Mask

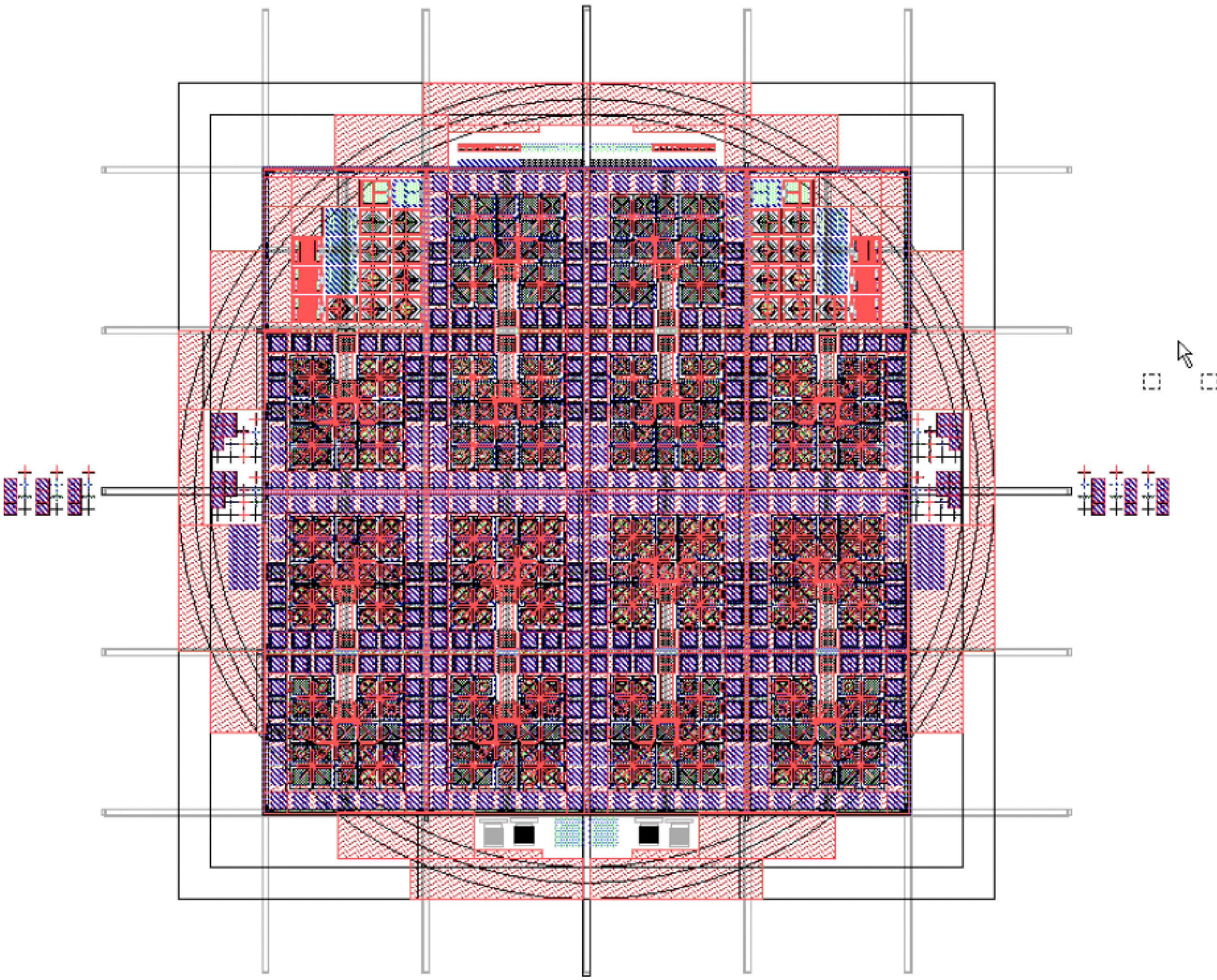

Chip Designs on the Wafer

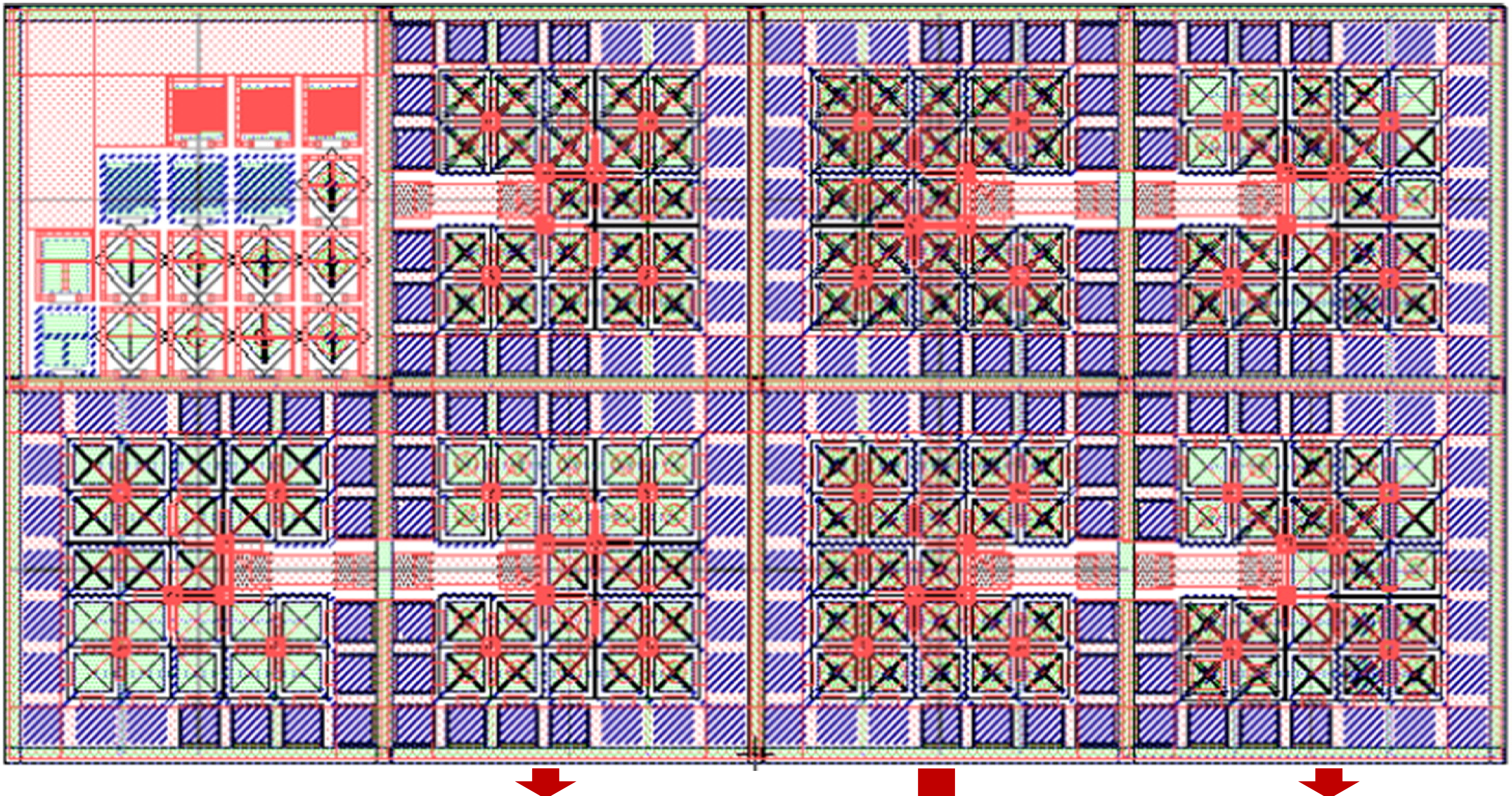

Resonator Size: 225 μm

Resonator Size: 150 μm

Resonator Size:75 μm

Zoom of One Chip

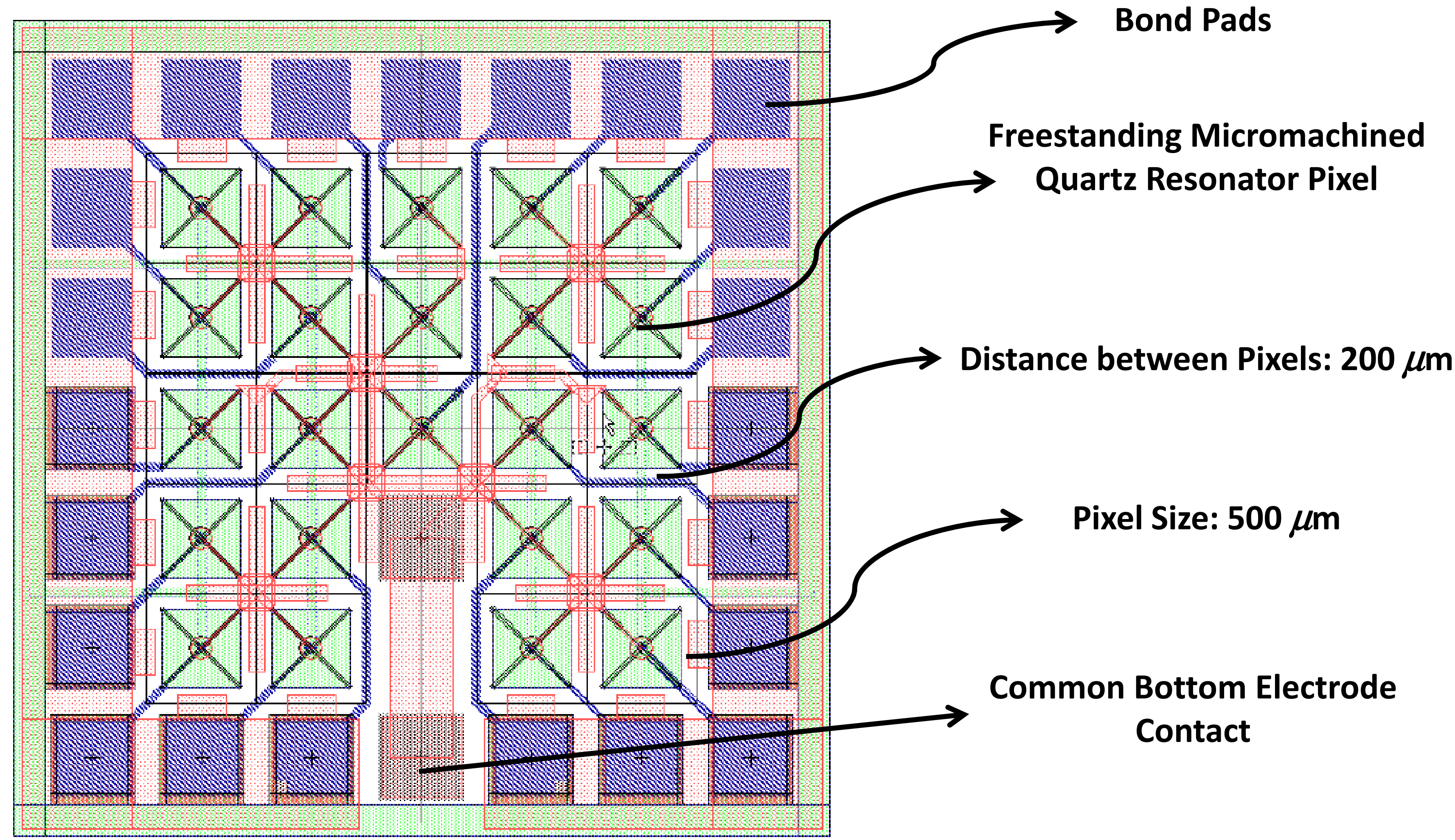

Details of Individual Pixel

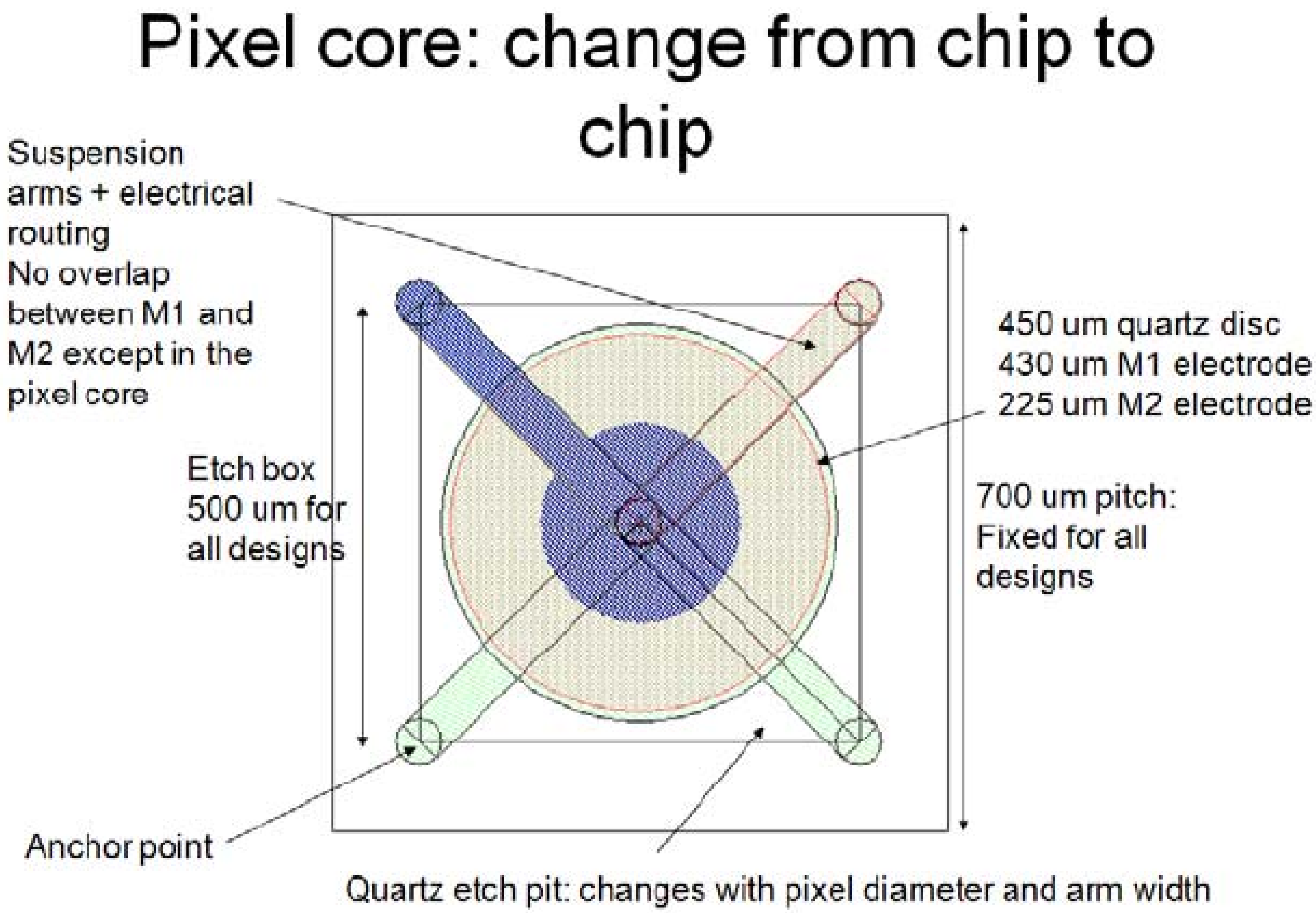

Fabrication Process Flow

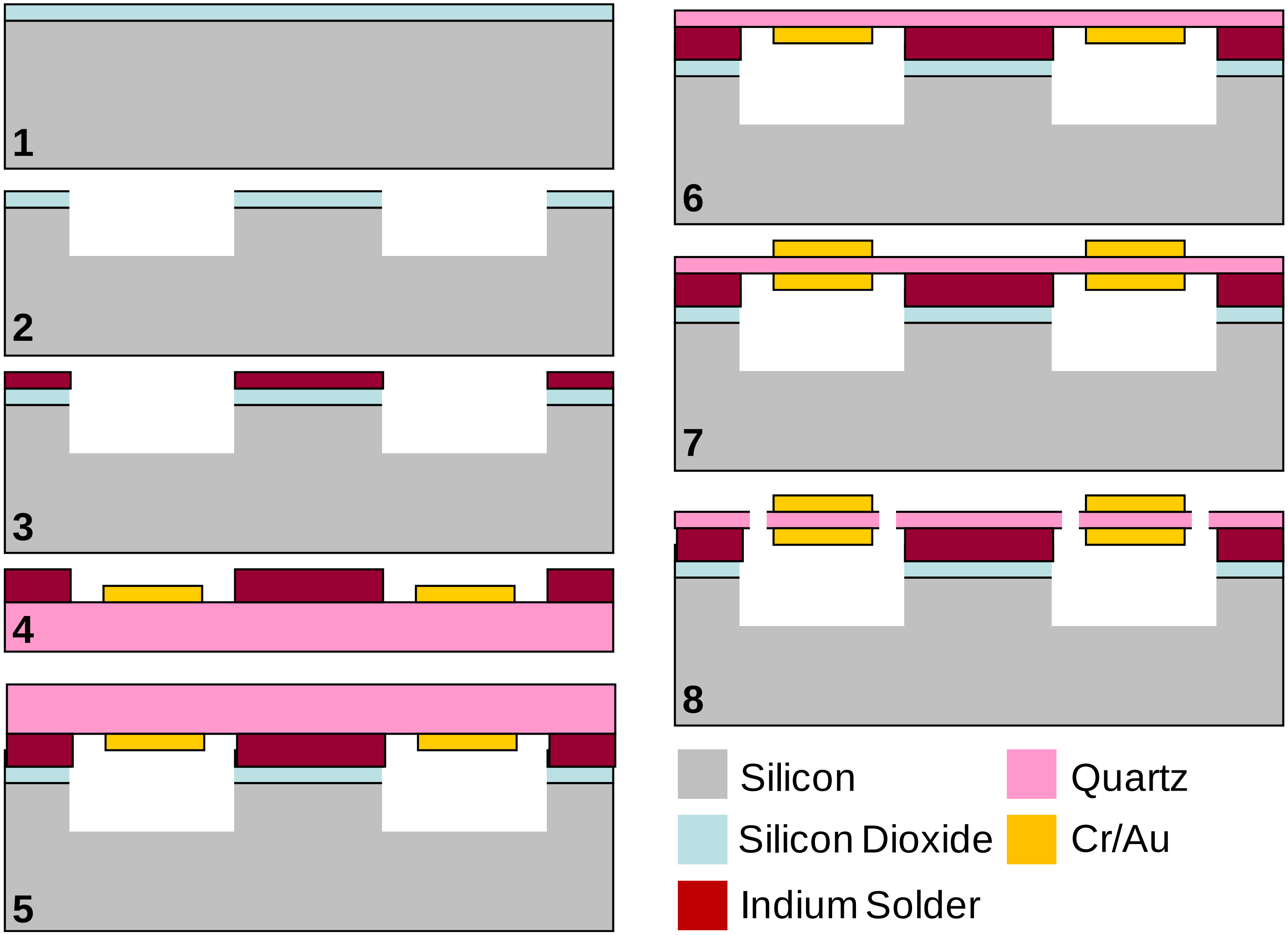

Fabricated Device Photos

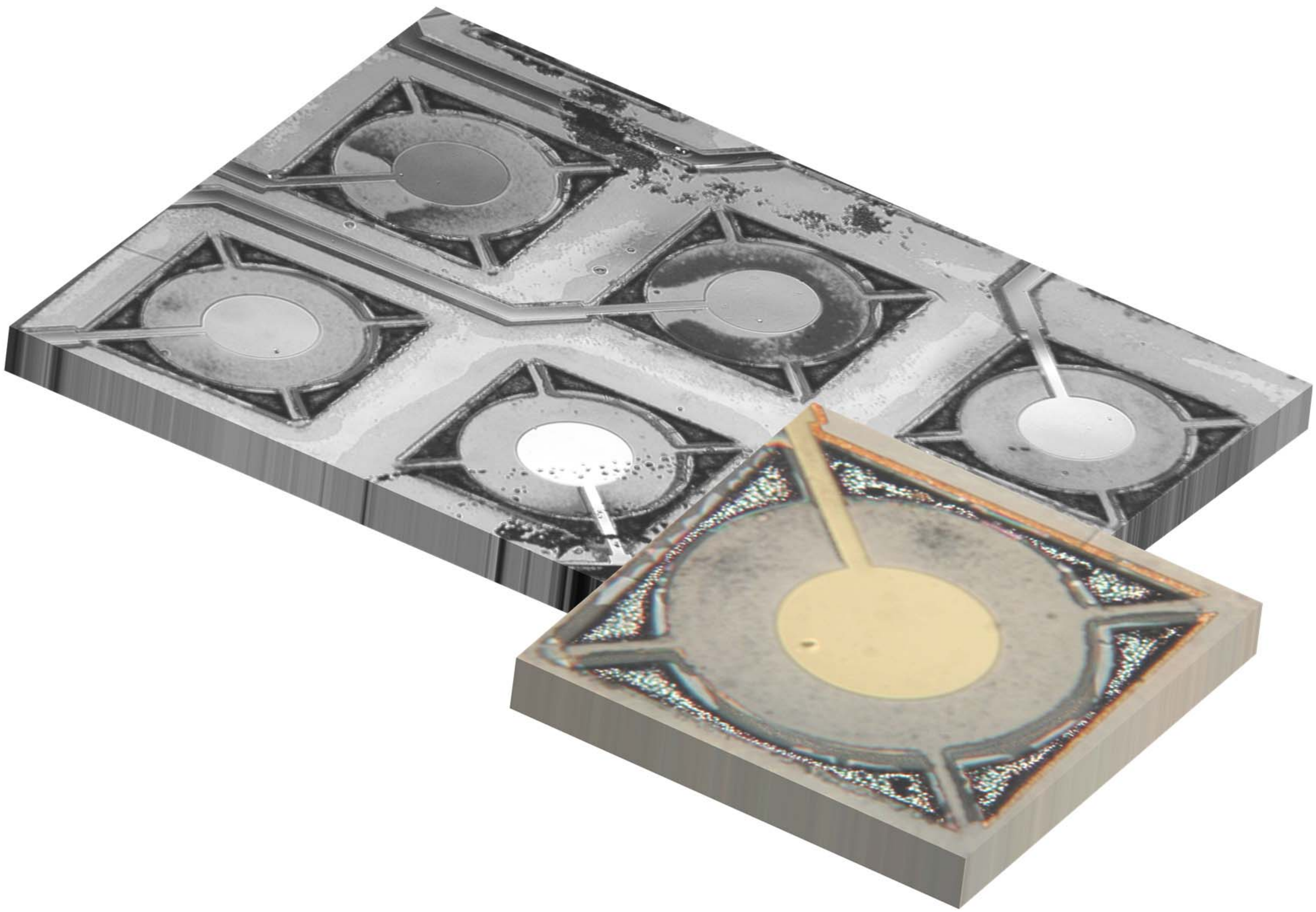

Resonance Characteristics

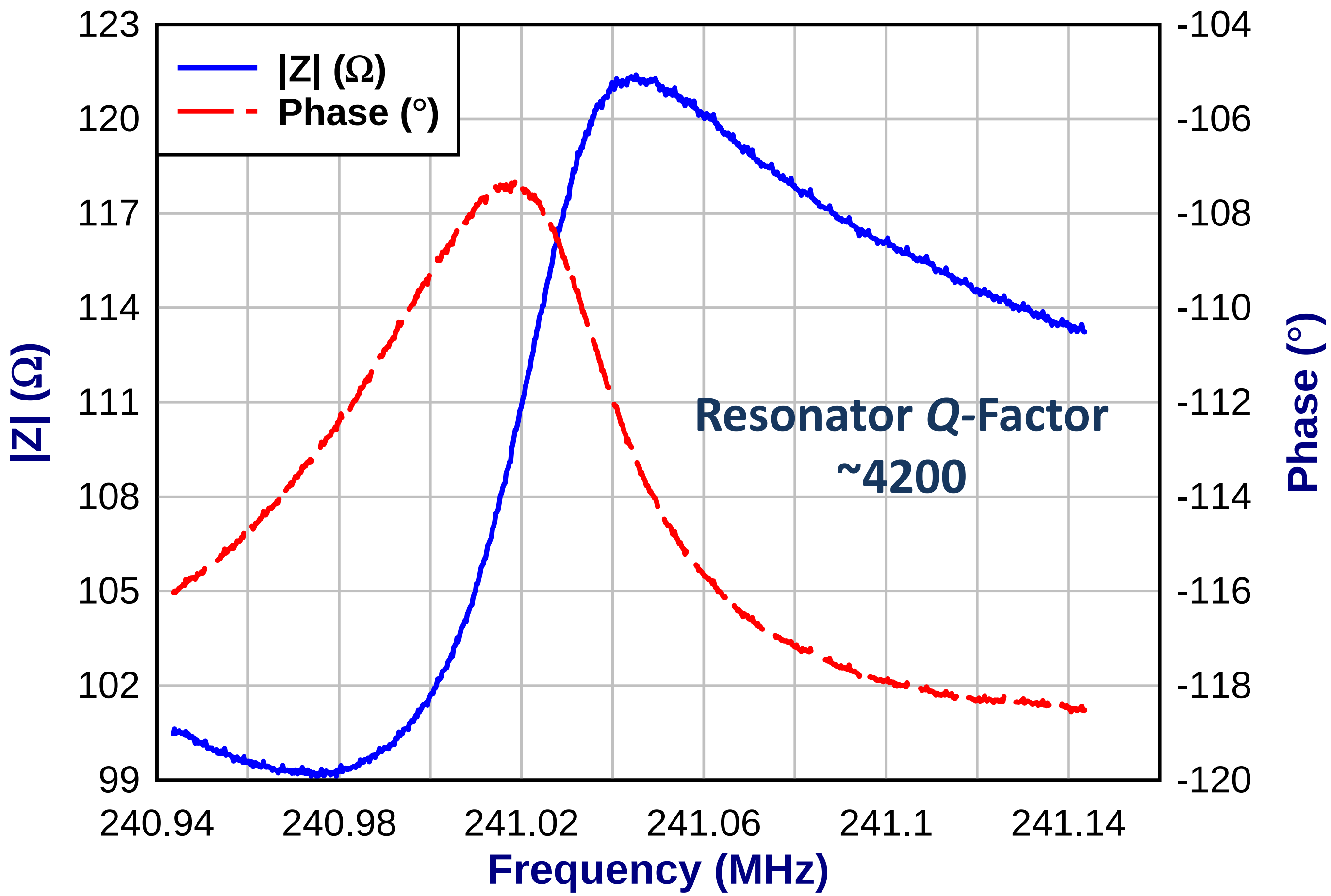

A resonance frequency of 241 MHz implies a resonator thickness of 6.9 μm.

Y-cut Quartz
Temperature Sensitivity of Resonance

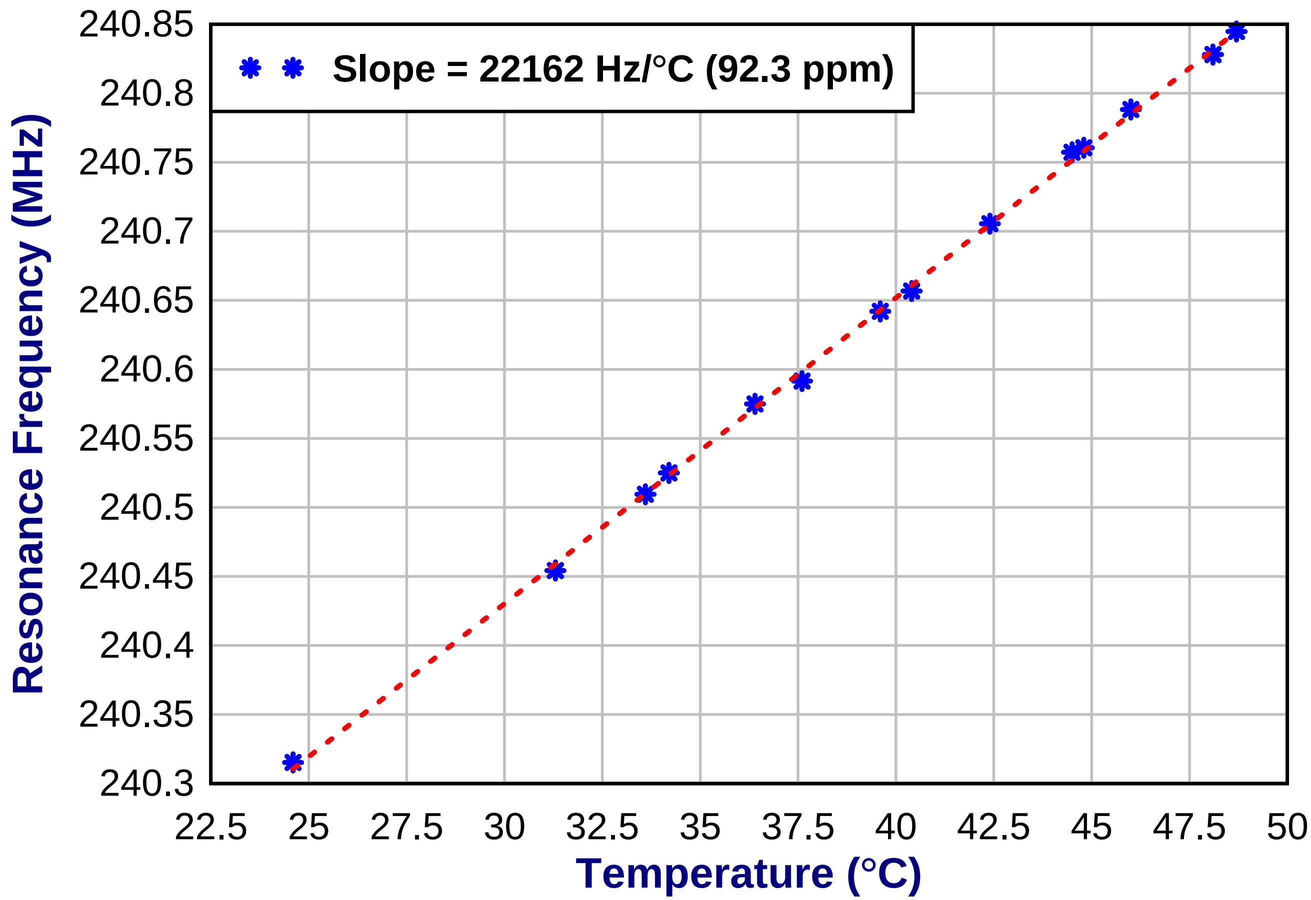

Measurement of Resonance Frequency Shift in Impedance Domain

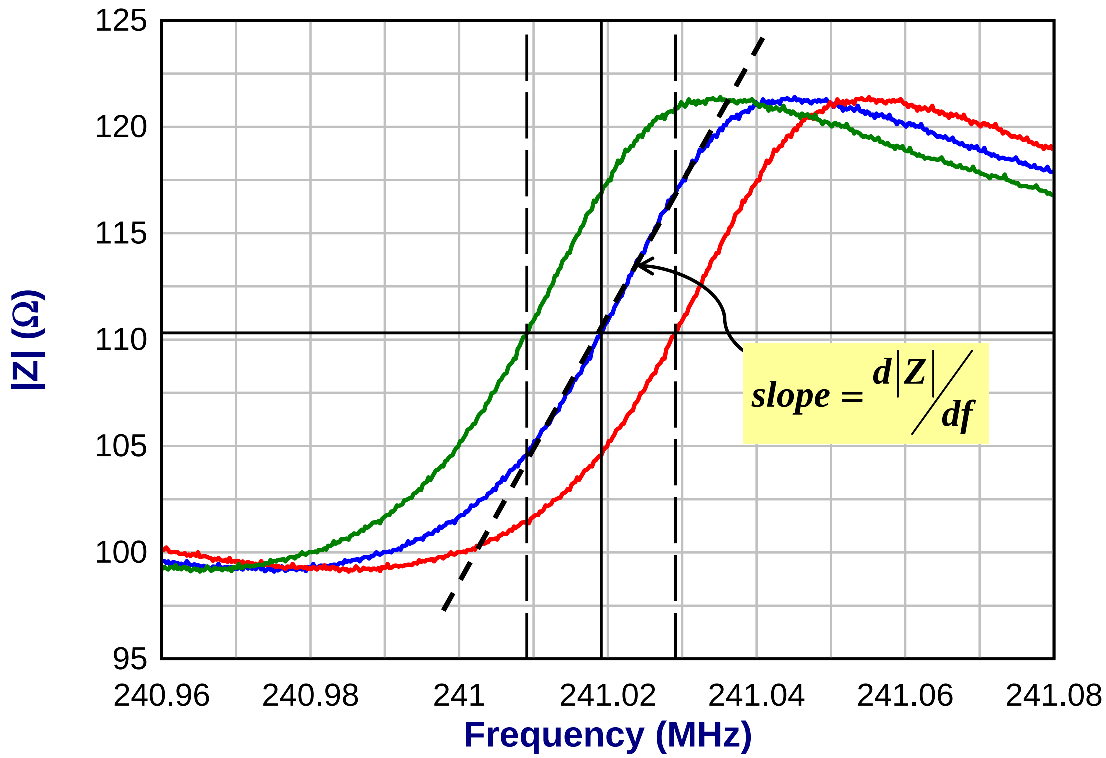

Normal sensing of the resonance curve involves measurement of the resonance frequency peak in real-time.

This temperature sensitivity of the measurement can be further enhanced as follows:

$$\boxed{\frac{d|Z|}{dT} = \frac{d|Z|}{df_0} \bullet \frac{df_0}{dT} = Slope \bullet \frac{df_0}{dT}}$$

For small frequency changes , the slope shown in the graph results in an additional gain in the measurement.

Monitoring the magnitude of the impedance of the resonator near its resonance at a fixed frequency operating point as the incident infrared radiation is modulated results in a modulation of the impedance – the magnitude of which is calibrated against a reference sensor.

Thermal and Infrared Characterization Measurement Set-up

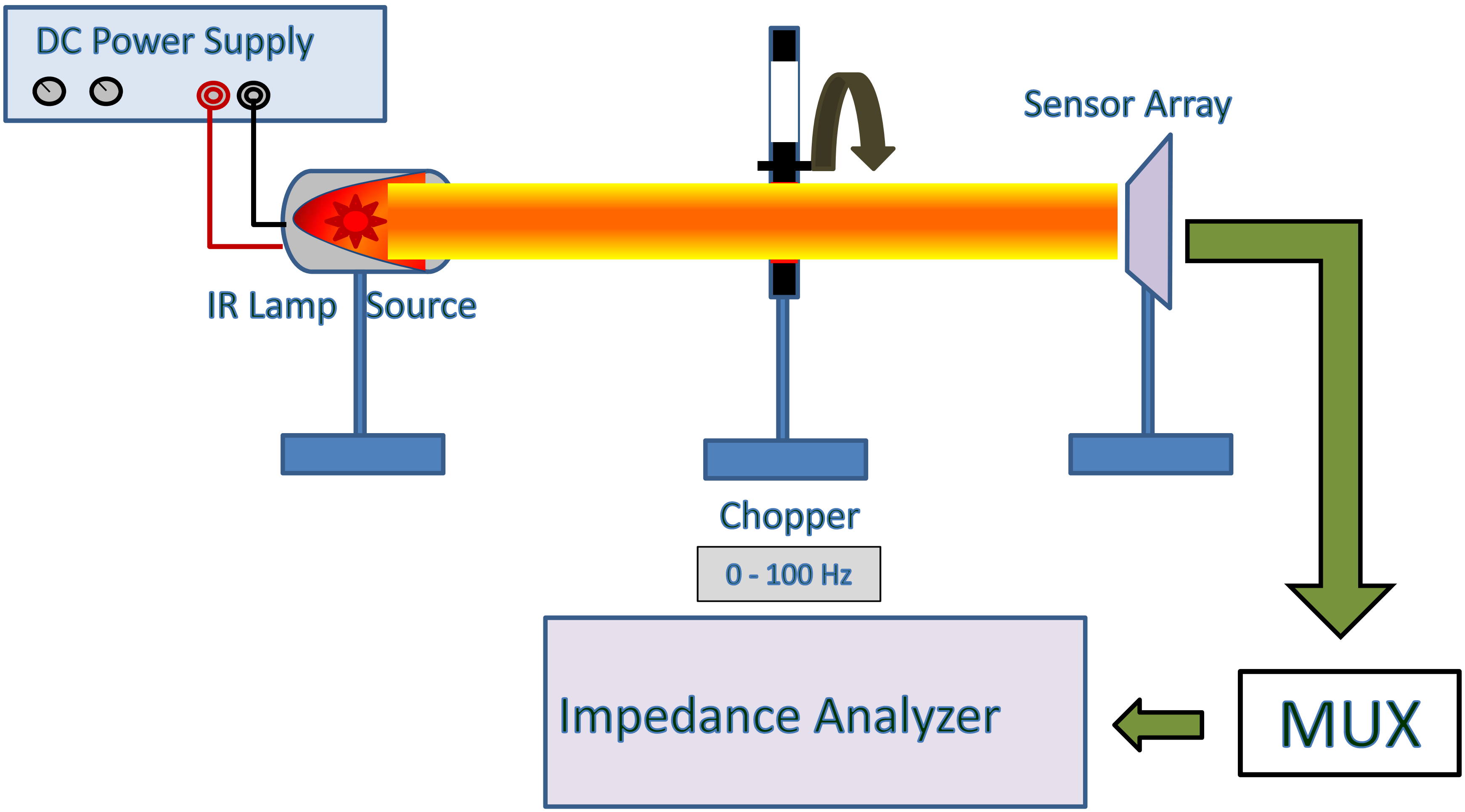

Thermal Response Time

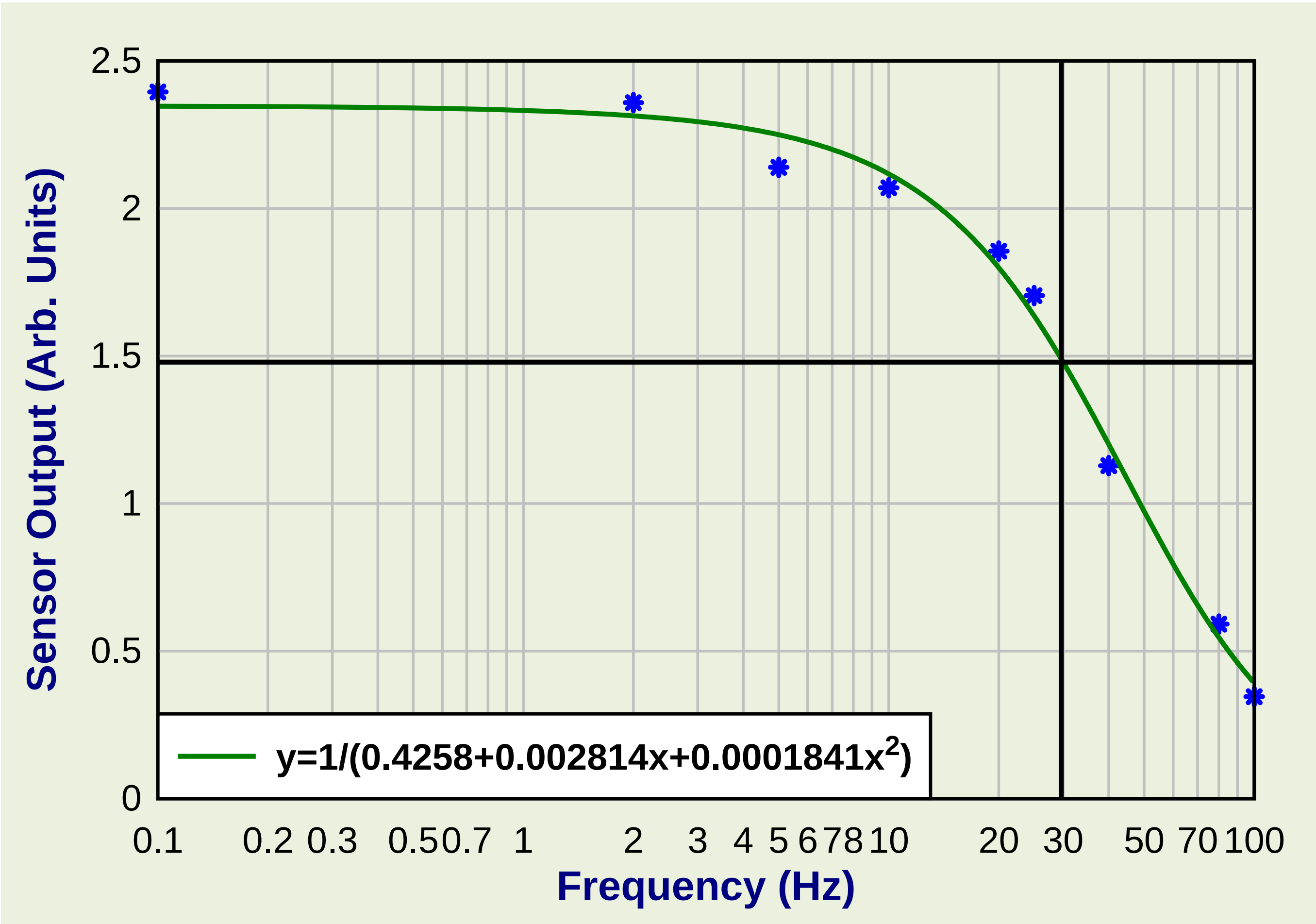

Sensor output at a given frequency divided by the output at DC for constant Lamp intensity is used to estimate the time-constant of the device.

Thermal Simulation

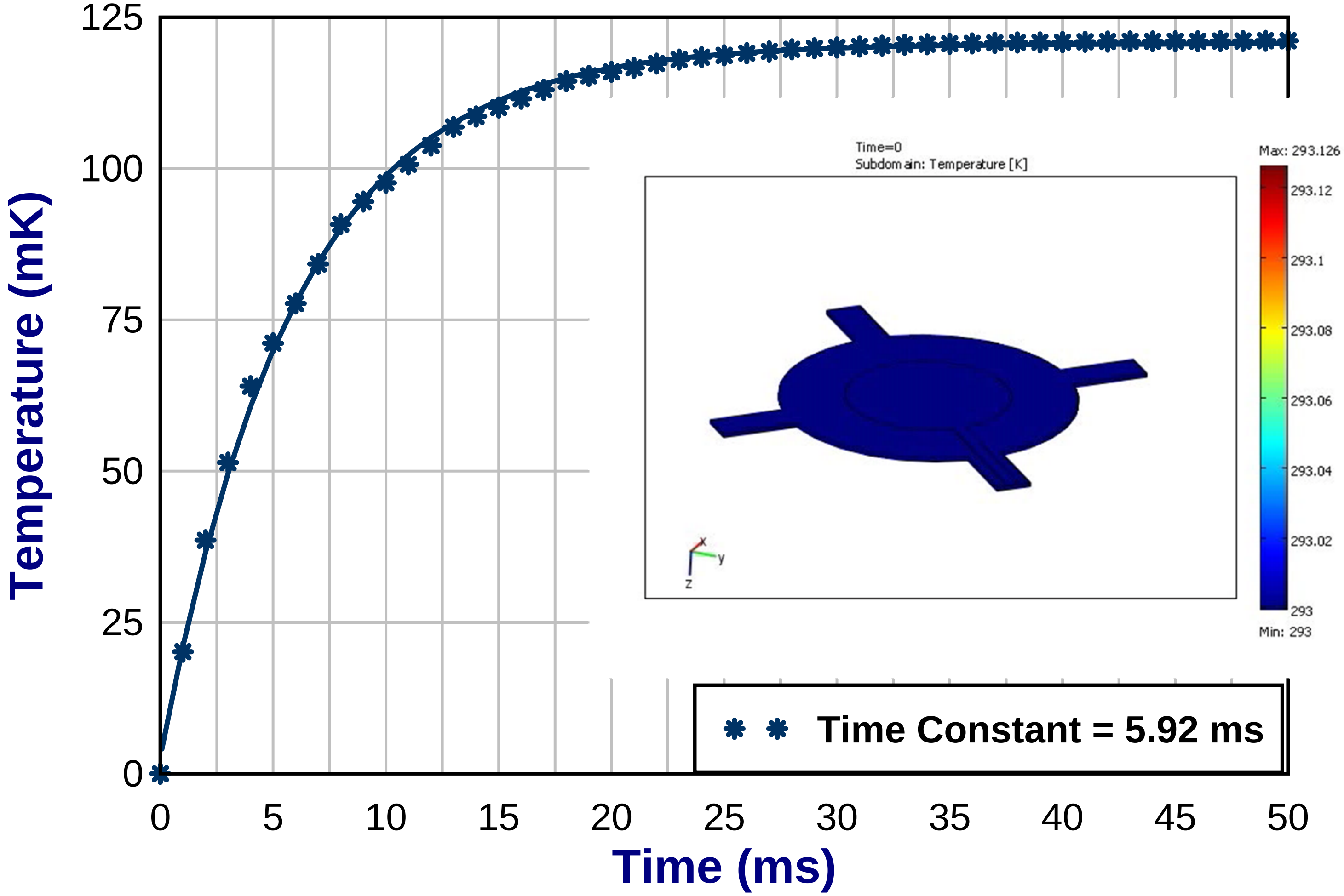

IR Response of the Quartz Resonator

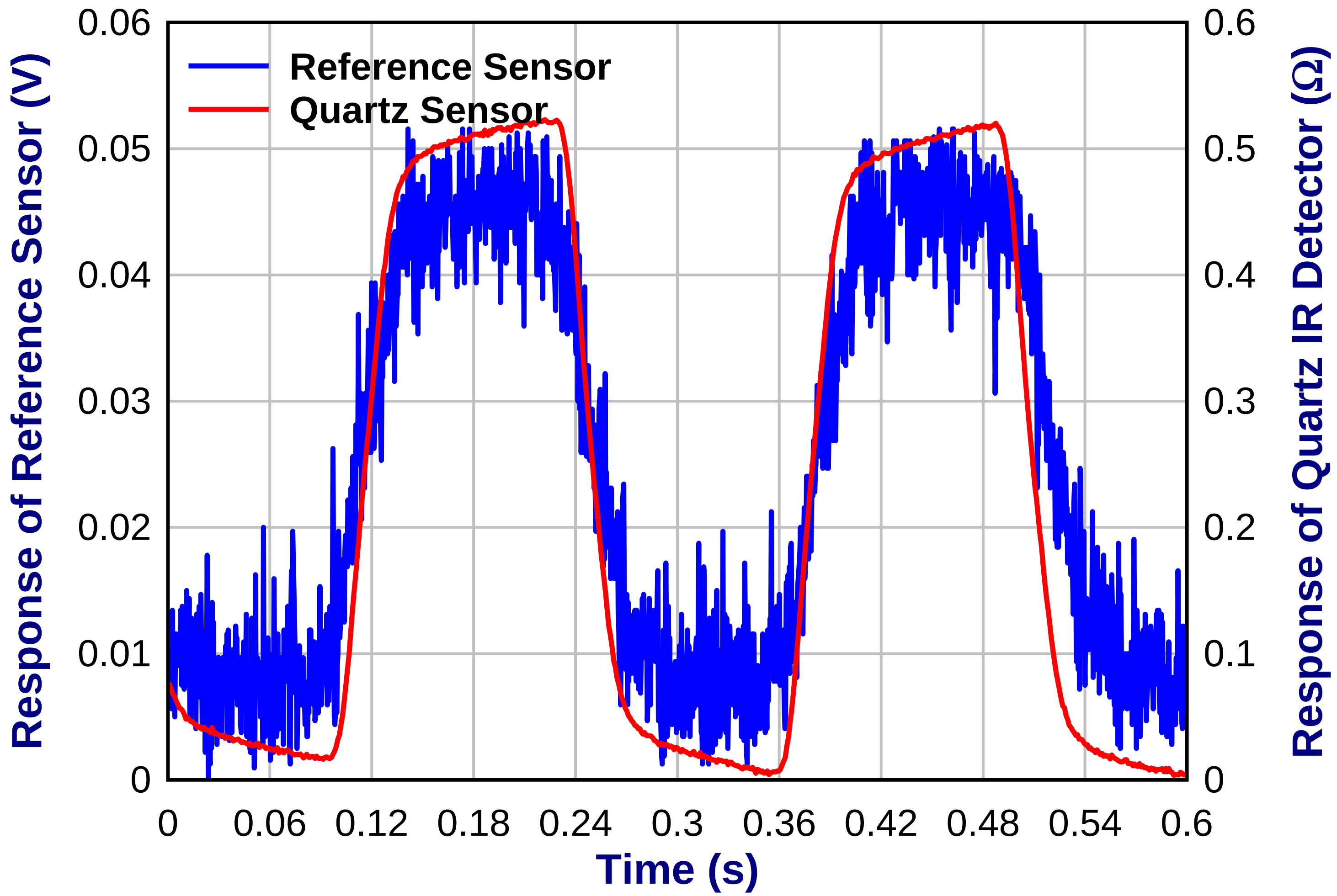

Summary

- At this point the 89 MHz and 241 MHz micromachined quartz resonators have been successfully fabricated and characterized.
- We have obtained good control over quartz etch rate and are able to successfully thin 100 μm thick quartz to 5 μm.
- The quality factor of the 241 MHz resonators fabricated using the new method is around 4200 and is largely affected by the parasitic coupling to the substrate silicon.
- The final through etch process to release the resonators has been improved to result in a high yield process.
- A new method to real-time track the resonance frequency of the Y-cut quartz sensors has been established.
- Initial testing of the IR detectors show very competitive performance in relation to the existing technologies. Quartz resonator based IR detectors are in principle capable of achieving background noise limited performance but need further research and development.
- A full patent based on the work in this project was filed through Penn State Intellectual Property Office.

Conclusions

- Micromachined Y-cut quartz resonators have been successfully fabricated with a fundamental resonance frequency of 240 MHz (6 μm in thickness)
- Temperature sensitivity of the sensors has been measured to 22.16 kHz/K!
- Fabricated resonators were tested for:
  - Responsivity: 7.32 kΩ/W
  - Noise Equivalent Power: 3.9 nW/$\sqrt{Hz}$
  - Response Time: < 30 ms
  - Noise Equivalent Temperature Difference: 4 mK
- Thermal models to explain the performance have been set-up.

PENNSTATE MEMS

Papers, Patents & Presentations

- **The following papers have been published:**
  - Ren K., Kao P., Pisani M.B., and Tadigadapa S. Monitoring biochemical reactions using Y-cut quartz thermal sensors, Analyst**, 136**, 2904 - 2911, **2011**.
  - Marcelo B. Pisani, Kailiang Ren, Ping Kao, and Srinivas Tadigadapa, Application of Micromachined *Y*-Cut Quartz Bulk Acoustic Wave Resonator for Infrared Sensing, Journal of Microelectromechanical Systems, **20(1)**, 288 - 296**, 2011.**
  - Kao, Ping, Tadigadapa, Srinivas, Micromachined quartz resonator based infrared detector array, Sensors and Actuators A: Physical, Vol. **149**(2), 189-192, **2009**
- **The following conference presentations have been made:**
  - Kailiang Ren, Marcelo Pisani, Ping Kao, and Srinivas Tadigadapa, Micromachined Quartz Resonator based High Performance Thermal Sensors, IEEE Sensors Conference, Waikoloa, Hawaii, November **2010**.
  - Marcelo B. Pisani, Kailiang Ren, Ping Kao, and Srinivas Tadigadapa, Room Temperature Infrared Imaging Array Fabricated Using Heterogeneous Integration Methods, Eurosensors XXIV, Linz, Austria, September **2010**.
  - Marcelo Pisani, Ping Kao, and Srinivas Tadigadapa, "Bulk acoustic wave resonators for infrared detection applications" Proceeding of IEEE Transducers, Denver, USA. **2009**.
- **The following invention disclosure has been made:**
  - Srinivas Tadigadapa and Marcelo Pisani, Fabrication Method and Detection Enhancement Strategy for Ultra-Sensitive Temperature Detection Using Resonant Devices, Invention Disclosure # P09582US01, submitted in **2011**.

PENNSTATE MEMS

Systematic Studies on Globular Proteins Using Micromachined High Frequency Bulk Acoustic Wave Resonators

Outline

- Why Quartz?
- Why miniaturize QCM?
- Micromachining Quartz
- Evaluation of QCM MicroArrays
- Adsorption Experiments
  - Human Serum Albumin, IgG, and Human Fibrinogen Adsorption on HD-SAMS
- Conclusions

PENNSTATE MEMS

Quartz Resonators: Motivation

ρ_q = 2648 kgm^{-3}

C_{66} = 2.947x10^{10} Pa

$$f_0 = \frac{\sqrt{c_{66}/\rho_q}}{2t_q}$$

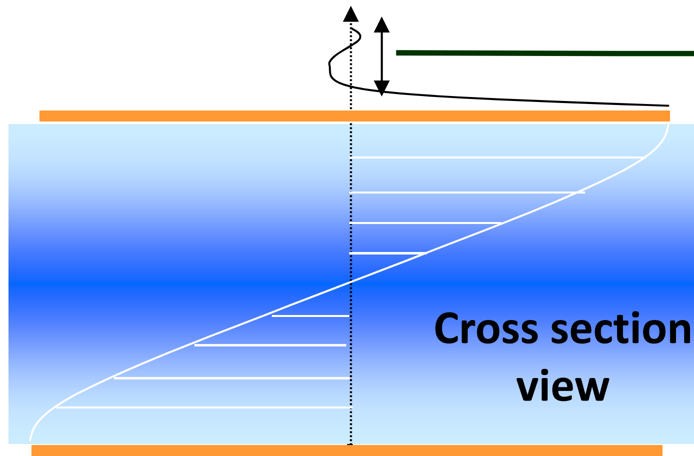

Decay Length

$$\delta = \sqrt{\left(\eta / \pi\rho f_0\right)}$$

Mass	Viscous	Viscoelastic
Sauerbrey equation, 1959	Kanazawa and Gordon, 1985	Martin, Kasemo, Hauptmann, 1996 - 2000
$\Delta f_s = -\left(2 f_0^2 / \sqrt{\mu_q \rho_q}\right)\Delta m = -S_f \Delta m$	$\Delta f_s = -\frac{f_s^{3/2}}{N}\sqrt{\frac{\rho\eta}{\pi\rho_q \bar{C}_{66}}}$	No Simple Equations Boundary Condition Dependent Solution
Thin, rigid, no slip condition	Semi-Infinite Newtonian fluid	Viscoelastic Layer in Liquids

Higher Sensitivity

Viscoelastic film

Decay length

Liquid viscosity

$$\delta = (\eta / \pi \rho f_0)^{1/2}$$

Resonance frequency

Liquid density

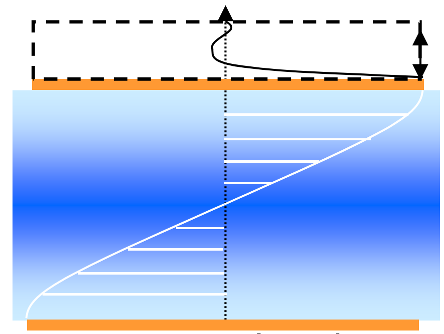

Cross section view

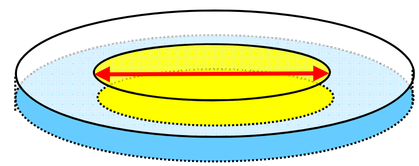

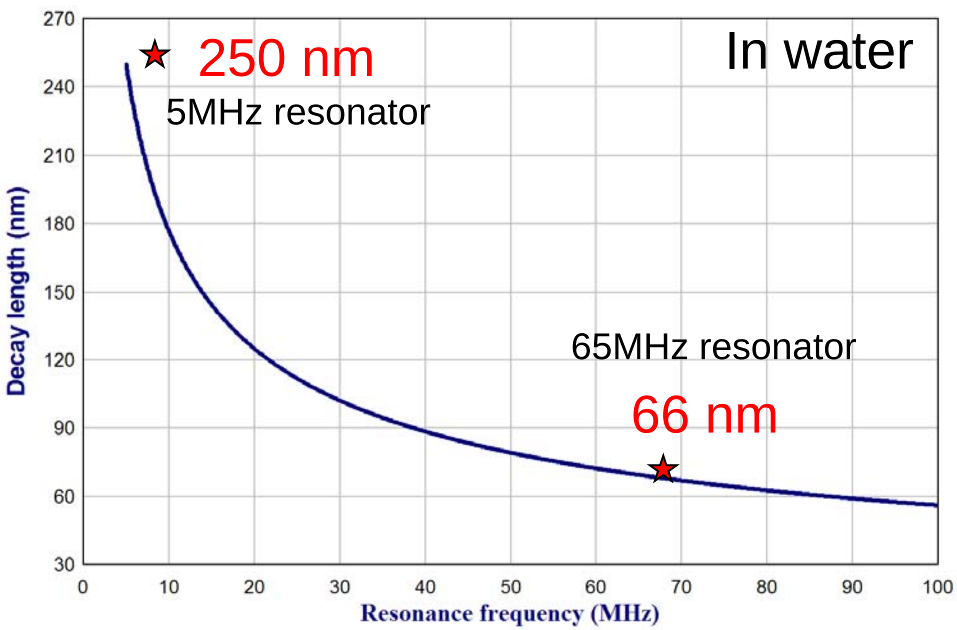

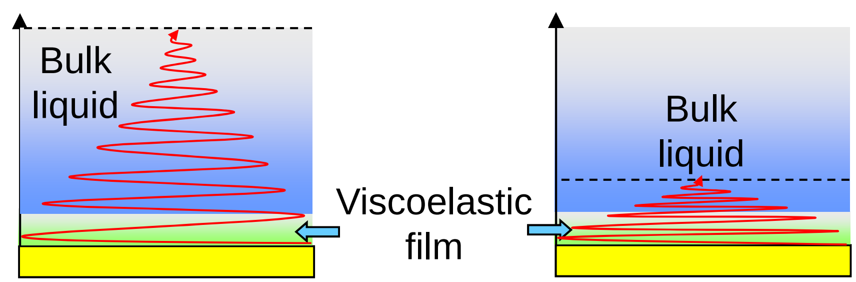

5MHz resonator

65MHz resonator

Resonator Response

35nm viscoelastic film

65MHz resonator

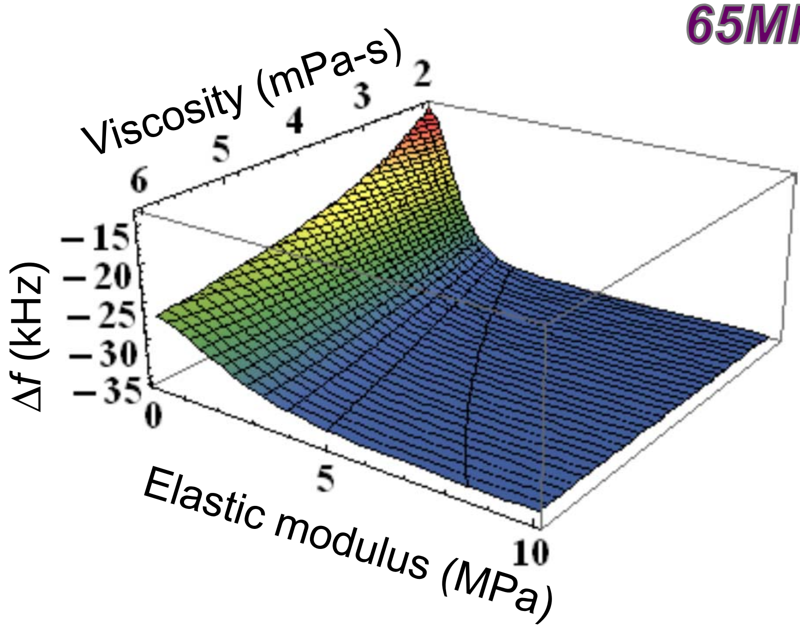

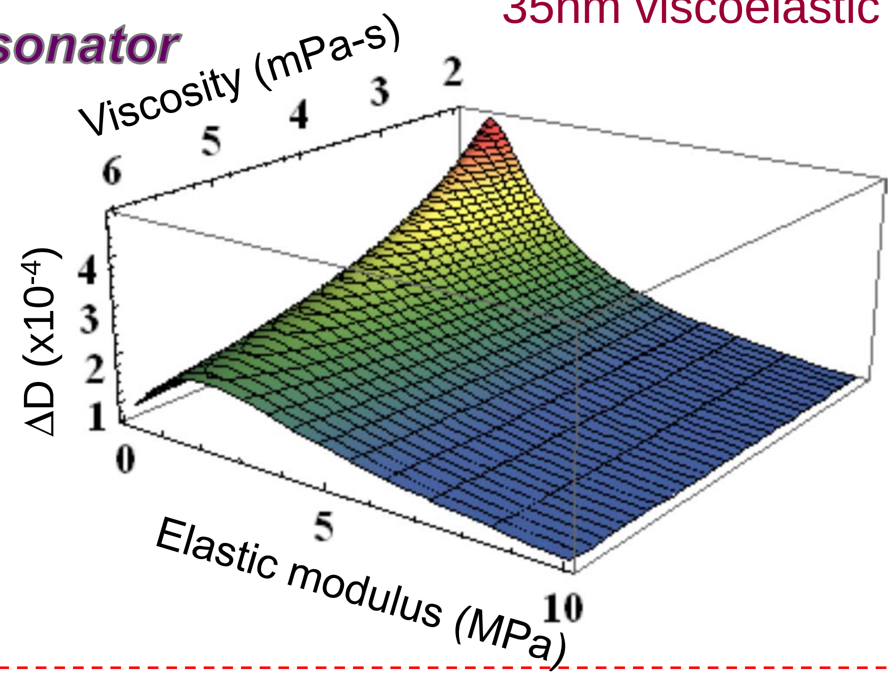

5MHz resonator

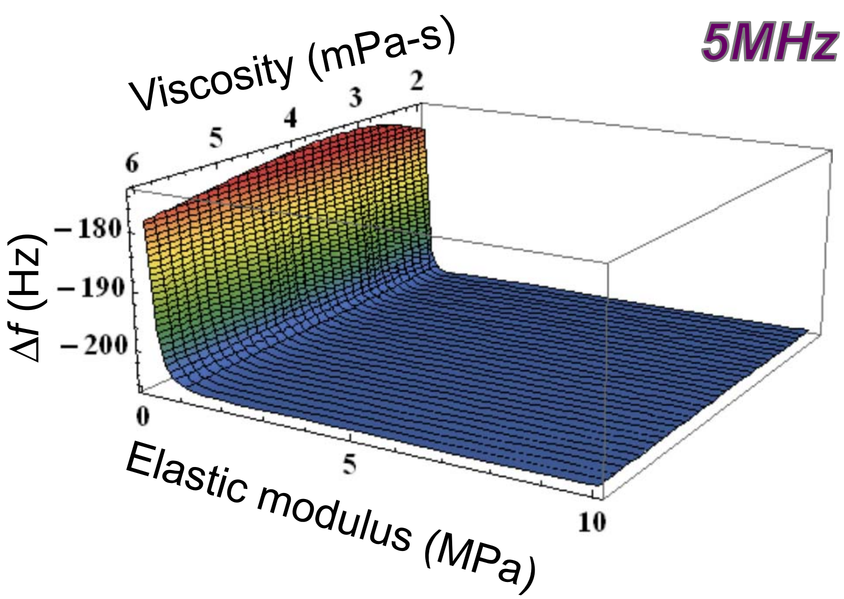

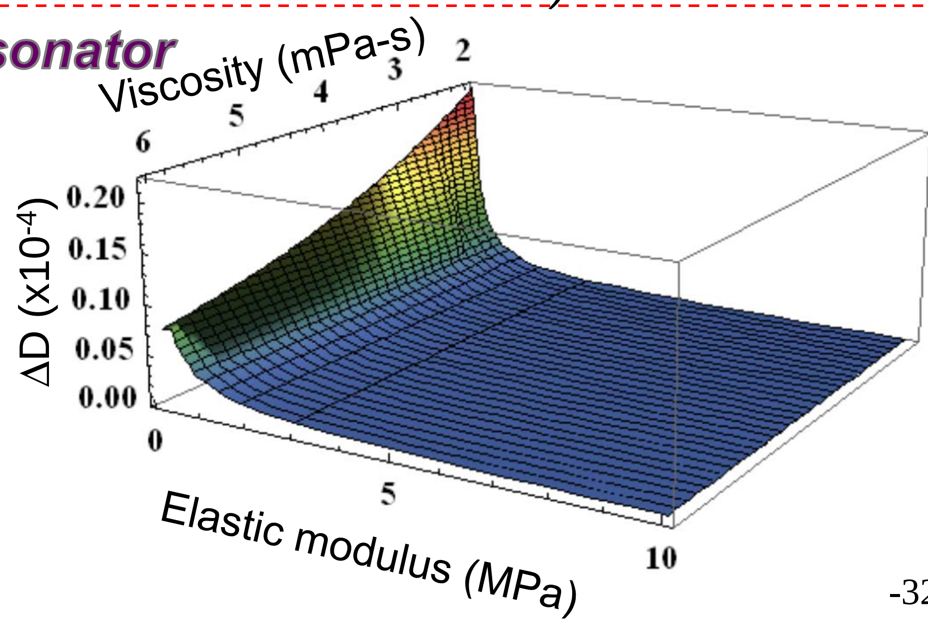

Fabrication of QCM Microarrays

PENNSTATE MEMS

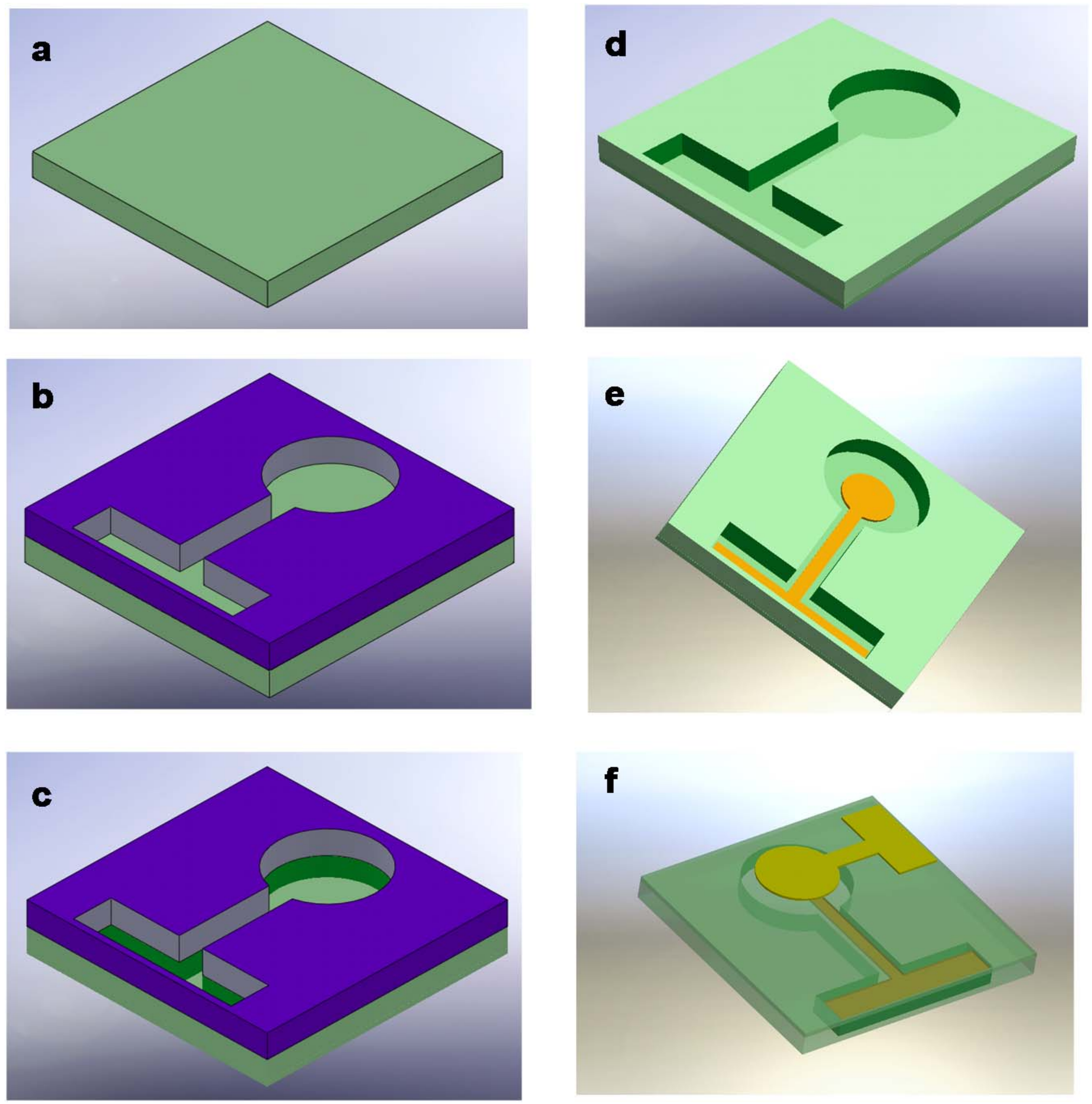

Design of the QCM Array

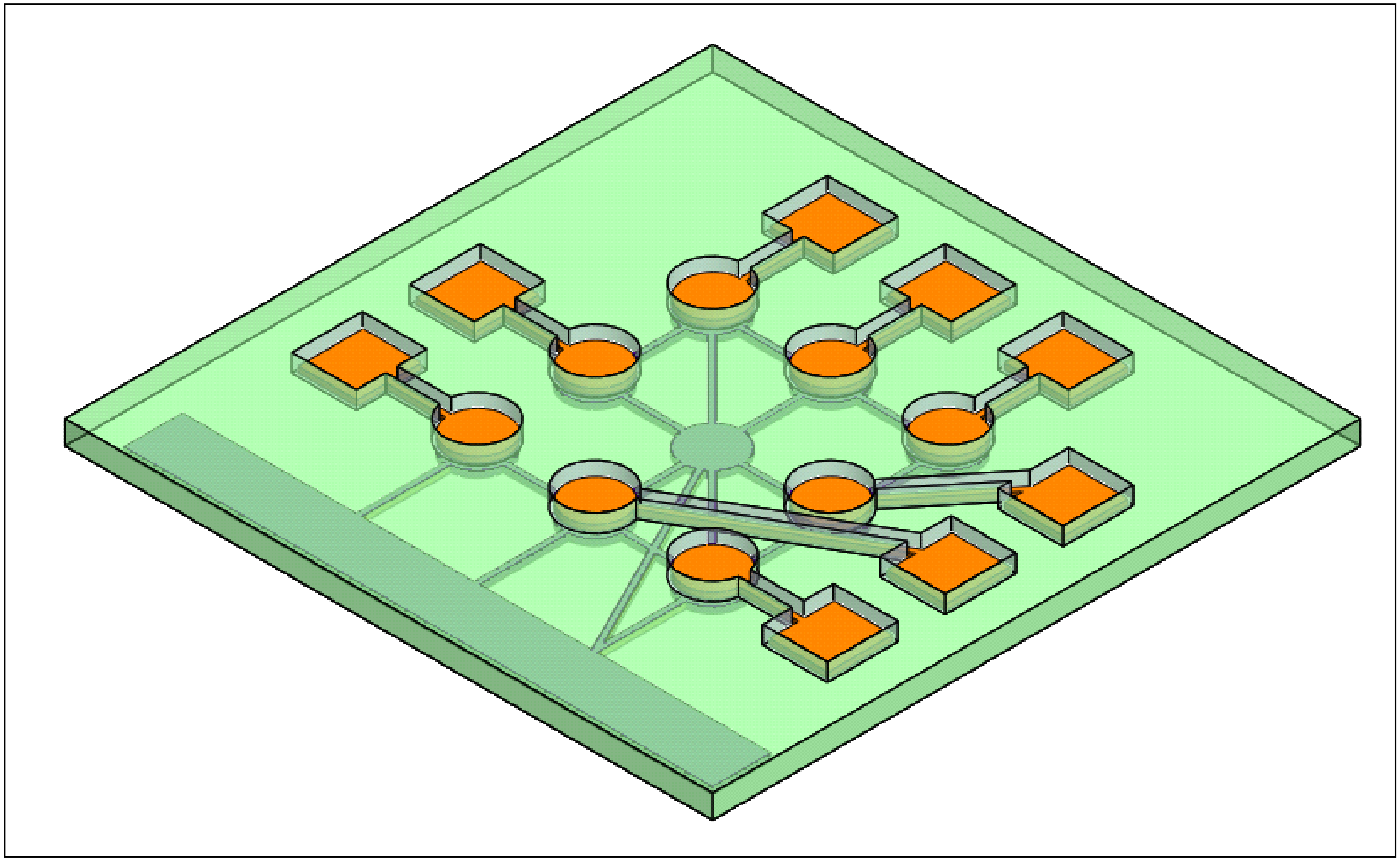

PENNSTATE MEMS

Fabricated & Packaged Device

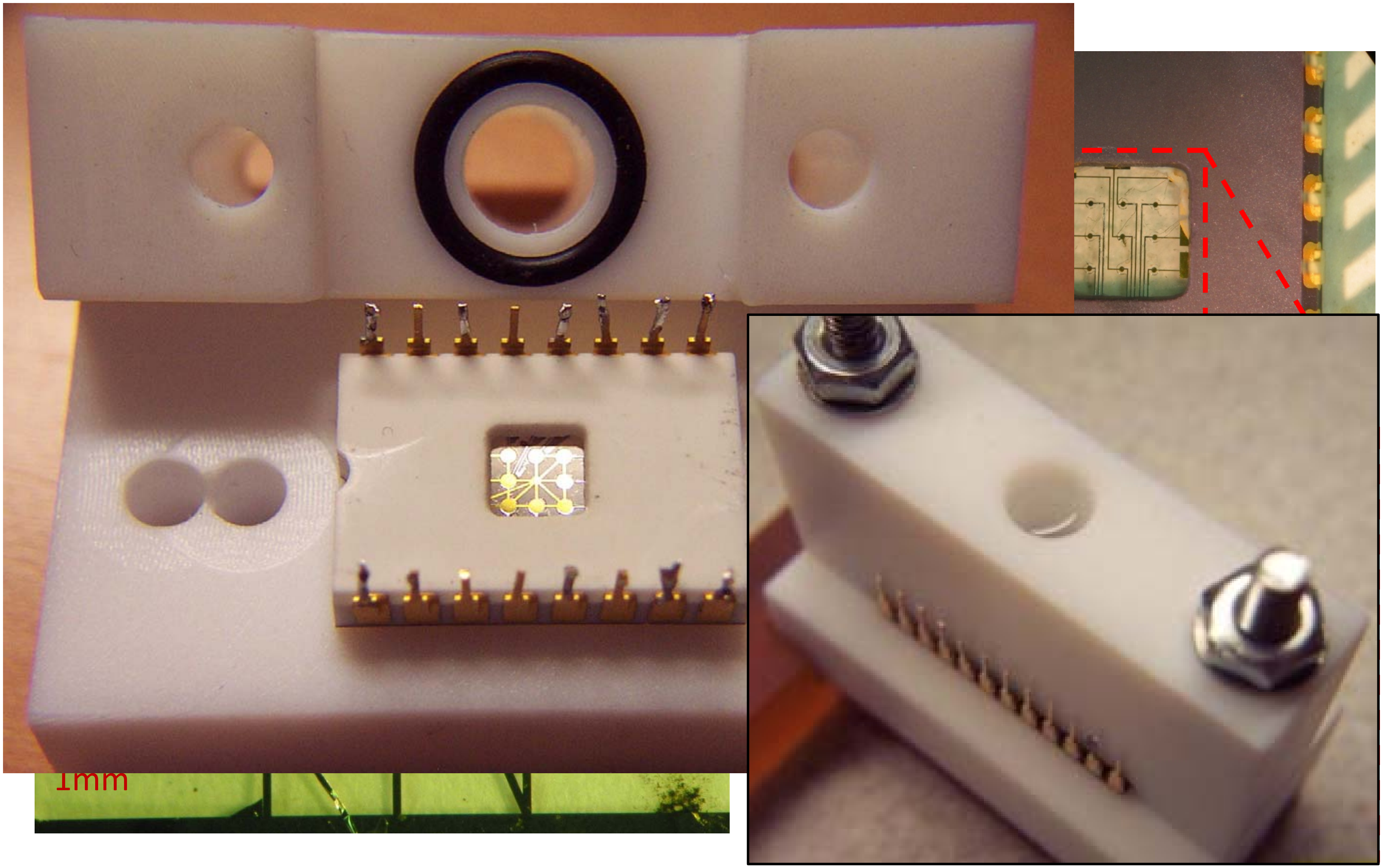

Interfacial layers studies

Globular proteins adsorption isotherm

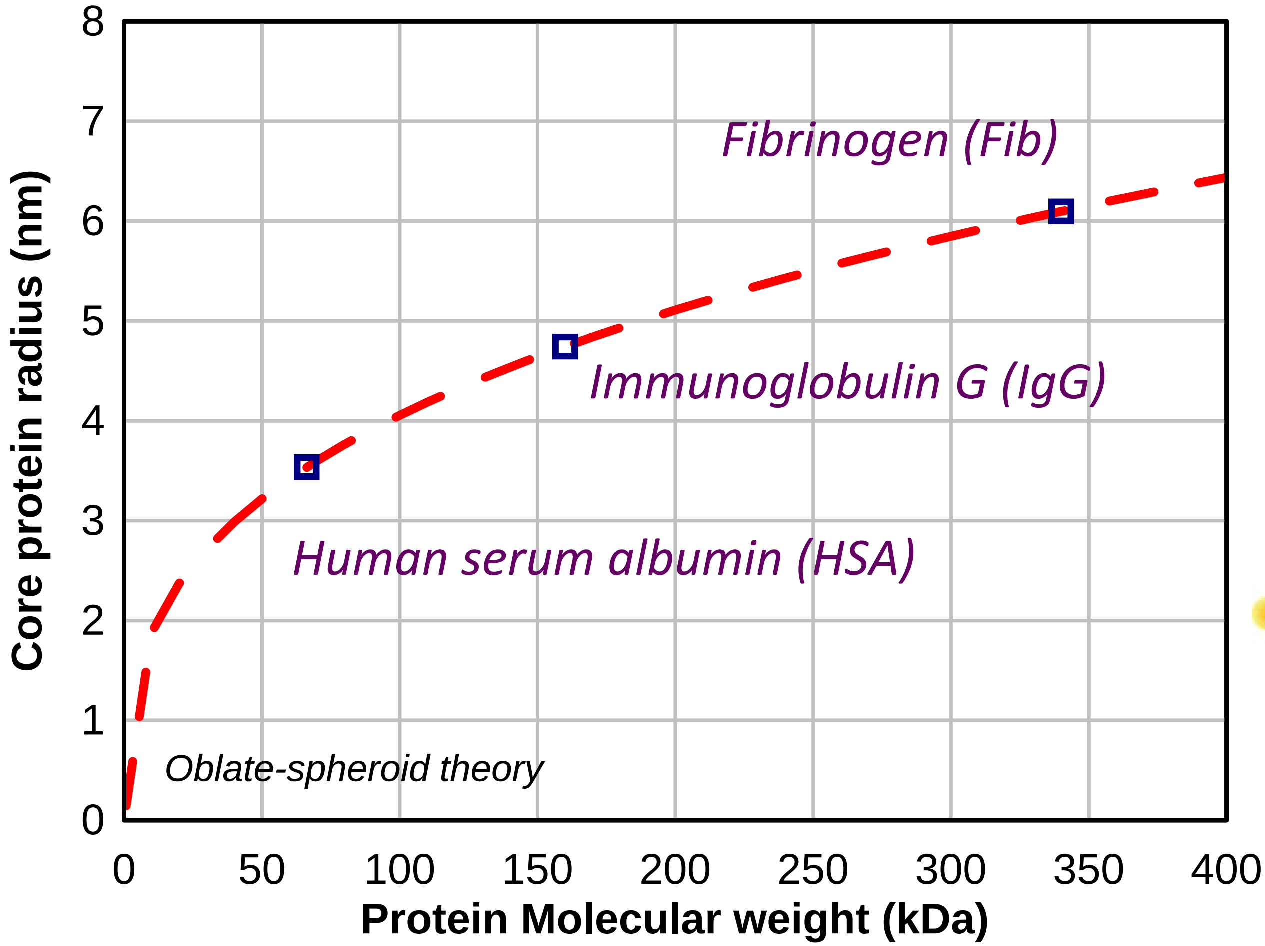

Artificial materials
-Hydrophobic surface

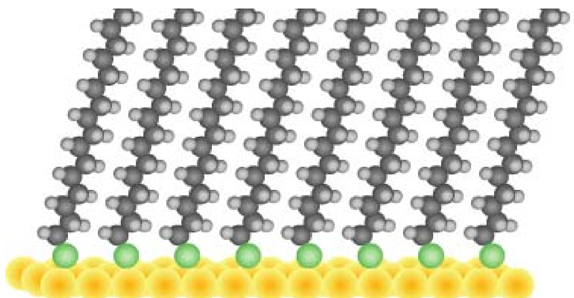

Hexadecanethiol
$CH_3(CH_2)_{15}SH$

C. Tanford, "How protein chemists learned about the hydrophobic factor," *Protein Science,* vol. 6, pp. 1358-1366, 1997.

Protein Adsorption Isotherm

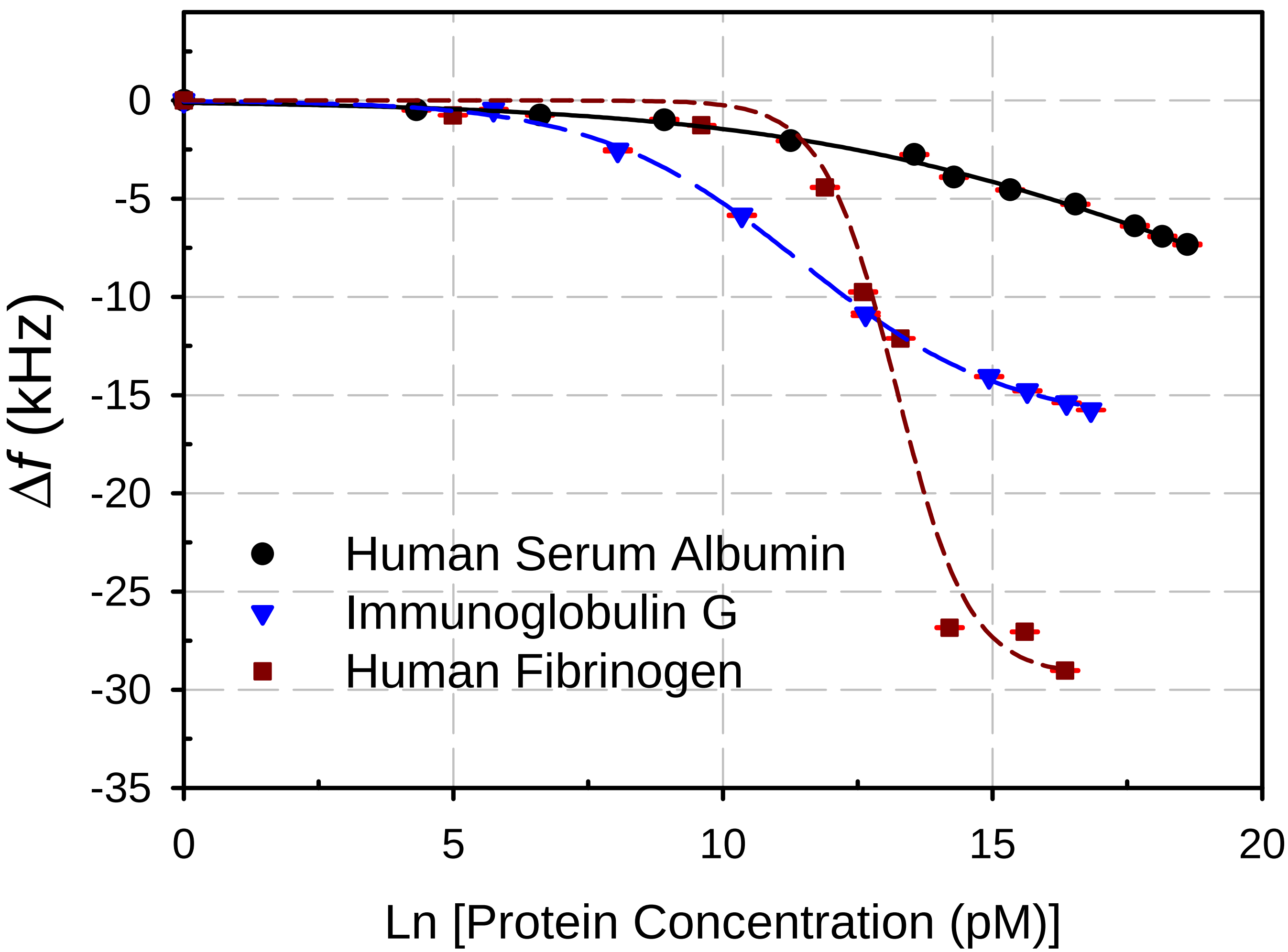

Langmuir Isotherms

The adsorption process between solution phase molecules, A, vacant surface sites, S , and the occupied surface sites, SA, can be represented by the equation

$$S + A \leftrightarrow SA$$

Assuming that there are fixed number of surface sites present on the surface, equilibrium coverage is independent of time and can be given by

$$\frac{\Gamma_{eq}}{\Gamma_{\max}} \Rightarrow \frac{\Delta m}{\Delta m_{\max}} \Rightarrow \frac{\Delta f}{\Delta f_{\max}} = \frac{KC}{1+KC}$$

where $K = k_+/k_-$ is known as the equilibrium adsorption constant., and C is the concentration of the adsorbate, Γ_{eq} and Γ_{max} are the equilibrium and maximum surface coverages respectively.

Rewriting:

$$\frac{C}{\Delta f} = \frac{C}{\Delta f_{\max}} + \frac{1}{K\Delta f_{\max}}$$

i.e. plotting $C/\Delta f$ as a function of C, the equilibrium association constant can be obtained.

Equilibrium Constant

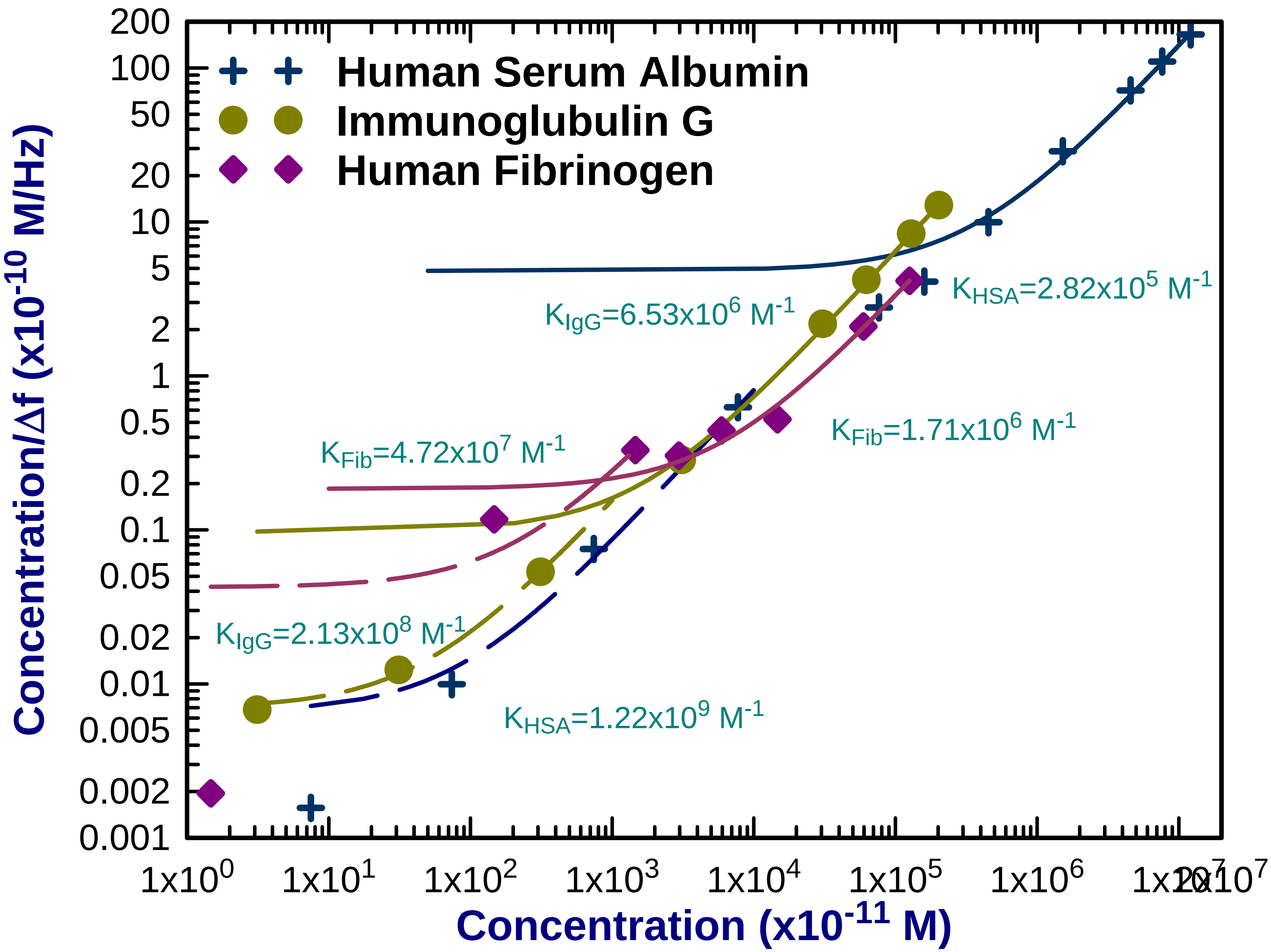

Modeling Protein Adsorption on QCM

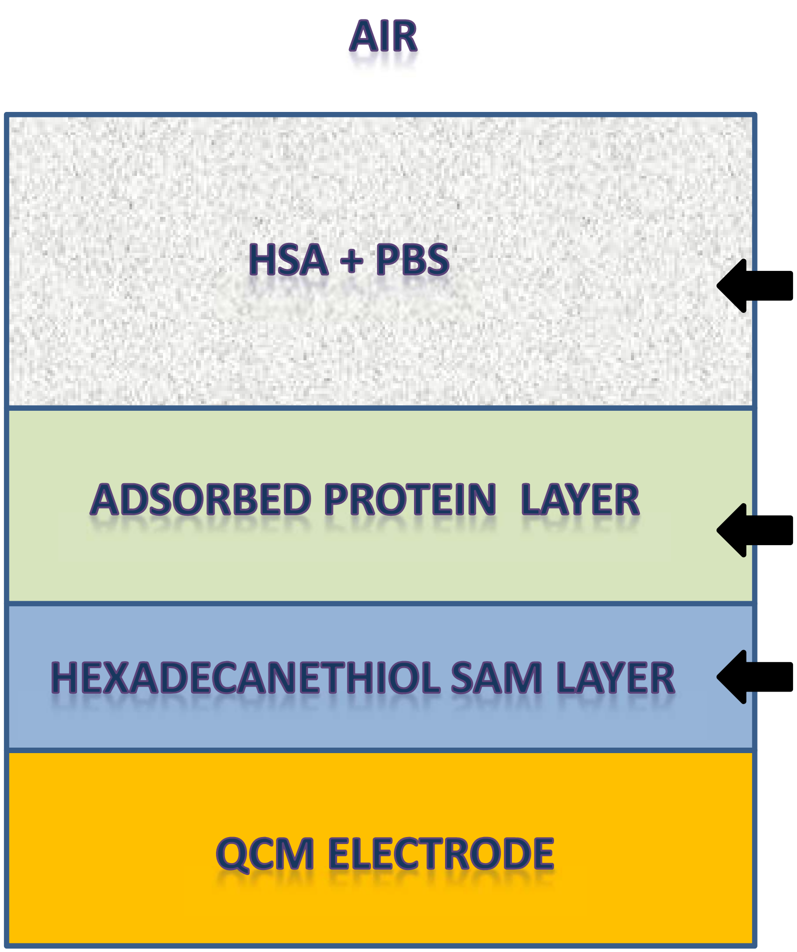

Modeled as **a Newtonian Fluid** characterized by viscosity η_L and density ρ_L.

Modeled as a **Viscoelastic Layer** characterized by a thickness t_F, density ρ_F, elastic modulus μ_F, and viscosity η_F.

Modeled as an **Ideal Mass Layer** of uniform density ρ

Modeling the Viscoelastic Layer

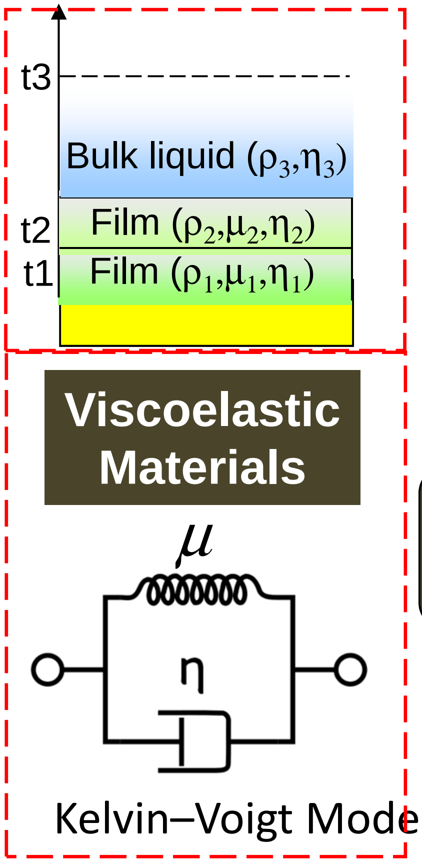

Measured

Frequency (f)
(1st mode)
(3rd mode)

Quality factor (Q)
(1st mode)
(3rd mode)

Four DATA

Δf_1 Δf_2
ΔQ_1 ΔQ_2

Simulation

Four Unknowns

t_{visc} :Thickness of film

μ_{visc} :Elastic modulus of film

ρ_{visc} :Density of film

η_{visc} :Viscosity of film

Kao, P., D. Allara, and S. Tadigadapa, Measurement Science & Technology 20(12)., 2009.

PENNSTATE MEMS

Modeling Protein Adsorption

- **Using Continuum Mechanics Approach, the solution for viscoelastic layers adsorbed in a Newtonian liquid can be given by:**

$$\Delta f \approx -\frac{1}{2\pi\rho_q t_q}\sum_{n=1,2,.}\left(t_n\rho_n\omega - 2t_n\left(\frac{\eta_{PBS}}{\delta_{PBS}}\right)^2\frac{\eta_n\omega^2}{\mu_n^2+\omega^2\eta_n^2}\right)$$

$$\Delta Q \approx -2\pi f_0\rho_q t_q\frac{\left[\sum_{n=1,2,.}\left(2t_n\frac{\mu_n\omega}{\mu_n^2+\omega^2\eta_n^2}\right)\right]}{\left[1+\sum_{n=1,2,.}\left(2t_n\left(\frac{\eta_{PBS}}{\delta_{PBS}}\right)\frac{\mu_n\omega}{\mu_n^2+\omega^2\eta_n^2}\right)\right]}$$

Subscripts *n* refer to the *n*th layer, PBS refers to the supernatant liquid layer (Phosphate Buffer Solution) in which protein adsorption experiments.

Voinova, Rodahl, Jonson, Kasemo, Physica Scripta, 1999. 59(5): p. 391
Kao, Allara, and Tadigadapa, Sensors and Actuators B, 142(2), 2009

Proteins Film Properties

	Thickness	Density	Viscosity	Modulus
HSA	7.5 (4*)	1100	3.5	1.8
IgG	18 (7.2**)	1040	5.5	6.7
Fib	37.5 (10***)	1100	2.7	0.42

( ) is the thickness of single layer

* Choi, E.J., et al., Langmuir, 2003. 19(13): p. 5464-5474. (Neutron reflectivity)

** C. Zhou, et al., Langmuir, vol. 20, pp. 5870-5878, Jul 2004 (Surface plasmon resonance (SPR))

*** R. J. Green, J. Davies, M. C. Davies, C. J. Roberts, and S. J. B. Tendler, Biomaterials, vol. 18, pp. 405-413, 1997. (SPR)

Theoretical Prediction

Proteins	Harmonic modes	Frequency Shift (kHz)		Q factor Change	
		Measured	Theory	Measured	Theory
HSA	1st mode	7.33	7.33	27	26
	3rd mode	14.04	17.02	100	91
IgG	1st mode	15.75	16.48	54	54
	3rd mode	43.39	47.20	254	258
Fib	1st mode	28.85	26.93	168	193
	3rd mode	56.85	57.43	490	469

Proteins Packing

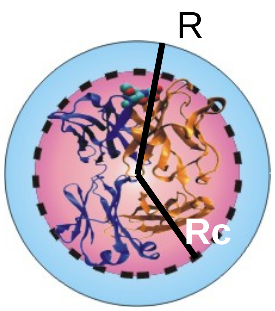

Oblate-spheroid theory

R is hydrated protein radius
Rc is the core protein radius

Proteins	MW (KDa)	Diameter of hydrated protein (nm) Theory	Thickness (nm) Measured	Assumed layer	Thickness per layer (nm) Measured
HSA	**66.3**	**7.1**	**7.5**	***1***	**7.5**
IgG	**160**	**9.5**	**18**	***2***	**9**
Fib	**340**	**12.2**	**37.5**	***3***	**12.5**

C. Tanford, *Protein Science,* vol. 6, pp. 1358-1366, 1997.

H. Durchschlag and P. Zipper, *Biophysical Chemistry,* vol. 93, pp. 141-157, 2001.

A. Krishnan, C. A. Siedlecki, and E. A. Vogler, *Langmuir,* vol. 19, pp. 10342-10352, 2003.

Dissipation factor

Dissipation factor = $1/Q$

Multiple slopes

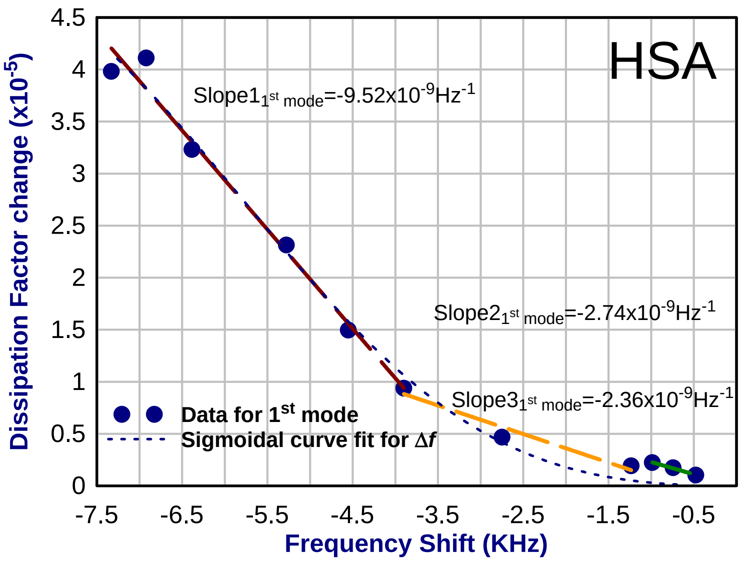

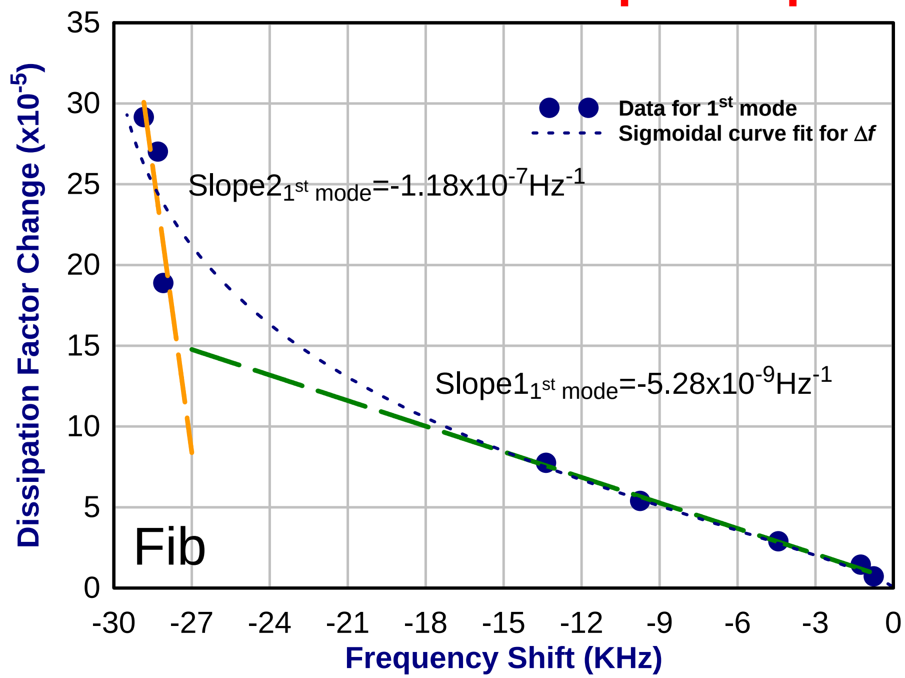

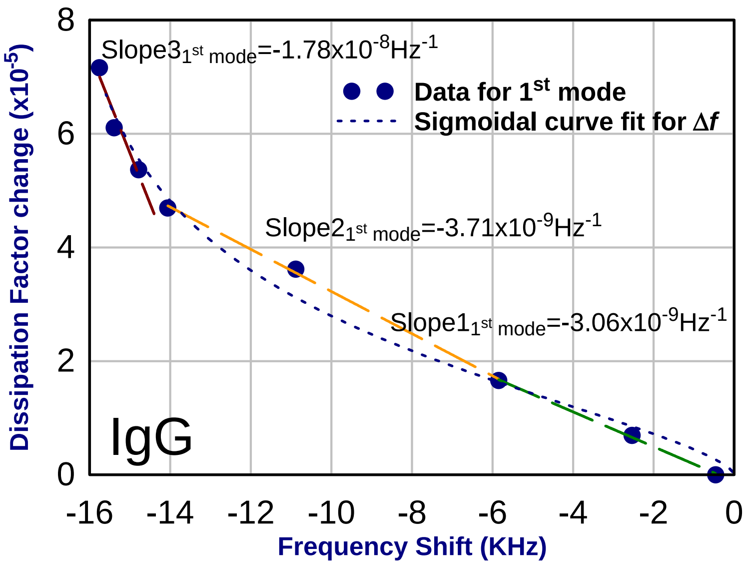

(10^{-9})	1st slope	2nd slope	3rd slope	High/low
HSA	2.36	2.74	9.52	**4**
IgG	3.06	3.71	17.79	**6**
Fib	5.27	117.5	N/A	**22**

Reorientation, Spreading, Conformation change

Sampling Volume

Single cell
Single resonator

Maxtek

Q-Sense

5MHz/ Diameter ~**7mm**

Minimum sample volume
~ 100µl for one resonator

$4800 USD (same experiment)

Multi cells
Multi resonators

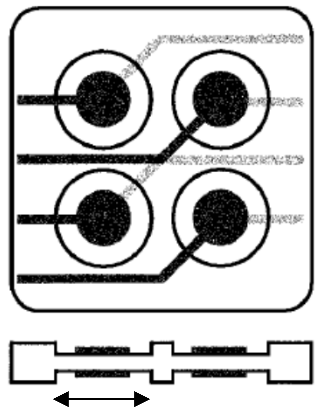

8 mm

10 MHz
Diameter ~**4.5mm**

Single cell
Multi resonators **(Array)**

25mm 25mm

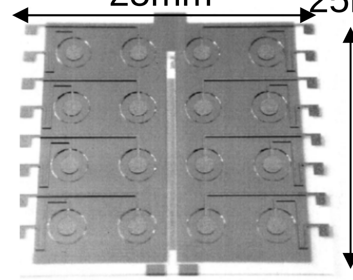

Post integrated
300µl for 16 resonators
50 MHz
Rabe et al

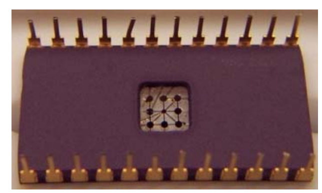

Our

9 mm x 9 mm

65~92 MHz/ Diameter ~**500µm**

Minimum sample volume
~ 20 µl for 8 resonators

$ 300 USD protein adsorption

http://q-sense.com/dbfiles/Q-Sense_E4%20Auto.pdf.

http://www.inficonthinfilmdeposition.com/en/maxtekrqcm.html

T. Tatsuma, Y. Watanabe, N. Oyama, K. Kitakizaki, and M. Haba, *Analytical Chemistry,* vol. 71, pp. 3632-3636, 1999.

J. Rabe, S. Buttgenbach, J. Schroder, and P. Hauptmann, *Ieee Sensors Journal,* vol. 3, pp. 361-368, 2003.

Conclusions

- Analysis of physical and viscoelastic properties
  - Thickness
  - Density
  - Viscosity
  - Elastic Modulus
- Sensitivity
  - Globular proteins
- Sampling volume
  - 8 resonators array type design (16 times reduction)

Thickness nm	Density kg/m^3	Visocsity mPa-s	Modulus (MPa)
<0.1nm	1.98	0.05	0.05

Quartz Crystal Resonator is not just a Microbalance!

Papers& Presentations

PENNSTATE MEMS

- **The following papers have been published:**
  - Kao P., Allara D., Tadigadapa S. Study of Adsorption of Globular Proteins on Hydrophobic Surfaces, IEEE Sensors Journal; **11(11)**, 2723 - 2731, 2011.
  - Ping Kao, Purnendu Parhi, Anandi Krishnan, Hyeran Noh, Waseem Haider,Srinivas Tadigadapa, David L. Allara, Erwin A.Vogler, Volumetric interpretation of protein adsorption: Interfacial packing of protein adsorbed to hydrophobic surfaces from surface-saturating solution concentrations, Biomaterials **32**, 969-978, 2011.
  - Ping Kao, David Allara, and Srinivas Tadigadapa, Fabrication and Performance Characteristics of High-Frequency Micromachined Bulk Acoustic Wave Quartz Resonator Arrays, Measurement Science and Technology, **20(12)**, 9pp, 2009.
  - Srinivas Tadigadapa and Kiron Mateti, Piezoelectric MEMS sensors: state-of-the-art and perspectives, Measurement Science and Technology, **20(10)**, 1-30, 2009.
- **The following conference presentations have been made:**
  - Hwall Min, Nichole Sullivan, David Allara, Srinivas Tadigadapa, Nanoporous Gold: A High Sensitivity and Specificity Biosensing Substrate, Eurosensors XXV, Athens, Greece, September 2011.
  - Hwall Min, David Allara, Srinivas Tadigadapa, Investigation of the Viscoelastic Properties of Liquids Trapped in Nanoporous Cavities using Micromachined Acoustic Transducers, Eurosensors XXV, Athens, Greece, September 2011.
  - Son Vu Hoang Lai, Ping Kao, Srinivas Tadigadapa, Thermal biosensors from micromachined bulk acoustic wave resonators, Eurosensors XXV, Athens, Greece, September 2011.
  - Ping Kao, David Allara, Srinivas Tadigadapa, Label free Piezoelectric DNA Sensor Arrays Using novel selective immobilization techniques, Proc. IEEE MEMS Conference, Cancun, Mexico, January 2011.
  - Ping Kao, Matthew P. Chang, David Allara, and Srinivas Tadigadapa, Investigation of Spontaneously Adsorbed Globular Protein Films using High-Frequency Bulk Acoustic Wave Resonators, IEEE Sensors Conference, Waikoloa, Hawaii, November 2010.
  - Ping Kao, Matthew P. Chang, David Allara, and Srinivas Tadigadapa, Systematic studies on globular proteins using micromachined high frequency bulk acoustic wave resonators, Eurosensors XXIV, Linz, Austria, September 2010.

PENNSTATE MEMS

High Speed Anisotropic Reactive Ion Etching (RIE) of Quartz and Pyrex Glass

Introduction

- Glass Etching: State of the Art
  - Background
  - Results from ICP-RIE Etching: Effect of various Process Parameters on Etch Characteristics
- Glass Etching: Issues
  - Masking Materials
  - Sidewall and Etch Pit Roughness
  - Wafer Mounting and Cooling
- Glass Etching: Future Directions

Requirements

- High Etch Rate
- High Anisotropy
- Planarity of Etched Surface
- Surface roughness control
- Optimum Properties of sidewalls
- High Selectivity

State of the Art

- Glass Etching/Shaping can be accomplished using
  - Wet Etching
  - Plasma Etching
  - Femtosecond Laser Micromachining
  - Other Creative Processing Methods

- TYPICAL COMPOSITION:
- PYREX
  - SiO_2 (80.6%), B_2O_3 (13.0%), Na_2O (4%), Al_2O_3 (2.3%), and K_2O (0.04%)
- BOROFLOAT
  - SiO_2 (81%) , B_2O_3 (13%) , Na_2O/K_2O (4%) , and Al_2O_3 (2%).

Wet Etching of Glass

Etchant	Etch Rate	Issues
HF (49%)[1]	1.32 – 3.2 μm/min	For Thermal Oxide, Masking
HF/HCl (10:1)[2]	7.86 μm/min	For Pyrex: Improved Roughness: 6nm

Typically in Pyrex Etching: Oxides, such as CaO, MgO or Al_2O_3, give insoluble products in HF solution: CaF_2 MgF_2 AlF_3

MASKING FOR WET ETCHING:
Photoresist: AZ 9260 – 3-4 minutes
Au/Cr: 10 – 14 minutes
PECVD Polysilicon (Annealed @ 400 C: over 30 minutes

1. K.R. Williams, R.S. Muller: Etch rates for micromachining processing, J. Micromech. Syst. 5(4), 256–269 (1996)
2. Ciprian Iliescua, Ji Jing, Francis E.H. Taya, Jianmin Miao, Tietun Sund: Characterization of masking layers for deep wet etching of glass in an improved HF/HCl solution, Surface & Coatings Technology 198 (2005) 314– 318

Laser Micromachining of Glass

Laser	Etch Rate	Issues
Excimer Laser	Channels of 100 µm width, 140 µm height and 4 mm length were written in 3 min using a spot size of 10 µm with an average power of 160 mW at 5 kHz, that is with a pulse energy of 0.0 32 mJ and a power of 0.27 GW (pulse duration of 120 fs).	Tapering Profile, Cracking, Serial Process

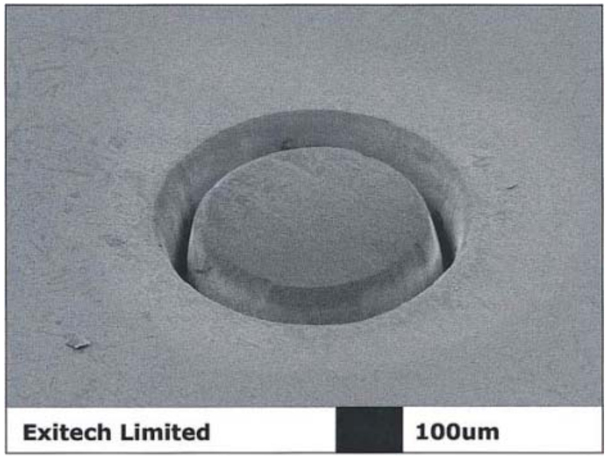

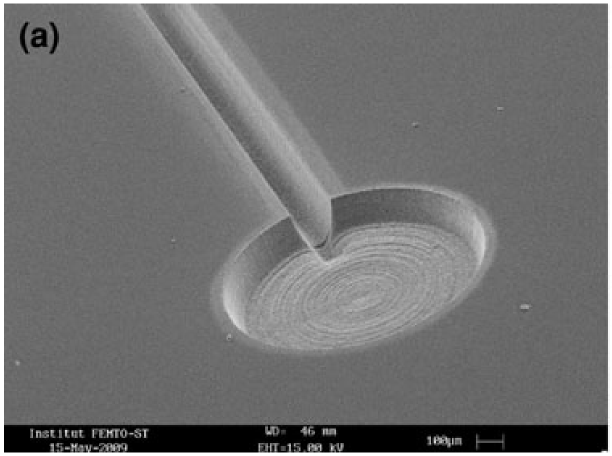

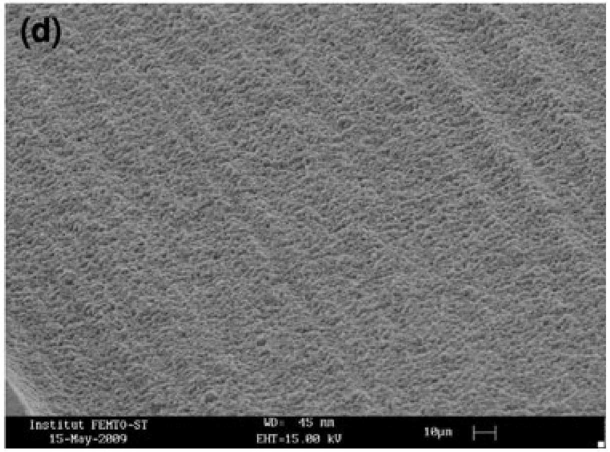

Typical Femtosecond Laser Characteristics: λ_0 ~800 nm, $\Delta\tau$ ~110 fs, E~1mJ/pulse, Rep Rate ~3– 5kHz

S. Queste, R. Salut, S. Clatot, J.-Y. Rauch, Chantal G, Khan Malek, Manufacture of microfluidic glass chips by deep plasma etching, femtosecond laser ablation, and anodic bonding, Microsyst Technol (2010) 16:1485–1493

Rafael R. Gattass and Eric Mazur, Femtosecond laser micromachining in transparent materials, nature photonics (2008) 2: 219-225

PENNSTATE MEMS

Quick Summary of Deep RIE of Glass

Reference	Mask type	Etching chemistry	Etching depth (μm)	Etching rate (μm/min)	Profile	Roughness Ra (nm)	Aspect ratio
Our work	Ni 8 μm	C_4F_8/O_2	120	1	83°–88°	2–10	40
Akashi and Yoshimura (2006)	Si wafer 200 μm	C_4F_8	430		80°		
Goyal et al. (2006)	Ni 5 μm	SF_6/Ar	20	0.536		1.97	
Ichiki et al. (2003)	Cr	SF_6	<20	1.2	88°	Very high	
Kolari et al. (2008)	Si wafer 400 μm	$C_4F_8/He/O_2$	250	0.5	80°–86°		<3
Kolari et al. (2008)	Si wafer 400 μm	$C_4F_8/He/O_2$	300	0.35			3
Kolari et al. (2008)	Ni 5 μm	C_4F_8/O_2	80	0.7	80°–86°		3.5
Li et al. (2001)	Ni	SF_6	200	0.6	88°	4	10
Park et al. (2005)	Ni	SF_6	40	0.75	<88°		
Park et al. (2005)	Ni	SF_6/Ar	27	0.54	88°		
Queste et al. (2008)	Ni 6 μm	C_4F_8/O_2	120	0.8	83°–88°	2	6

S. Queste, R. Salut, S. Clatot, J.-Y. Rauch, Chantal G, Khan Malek, Manufacture of microfluidic glass chips by deep plasma etching, femtosecond laser ablation, and anodic bonding, Microsyst Technol (2010) 16:1485–1493

ICP-RIE Set-up used

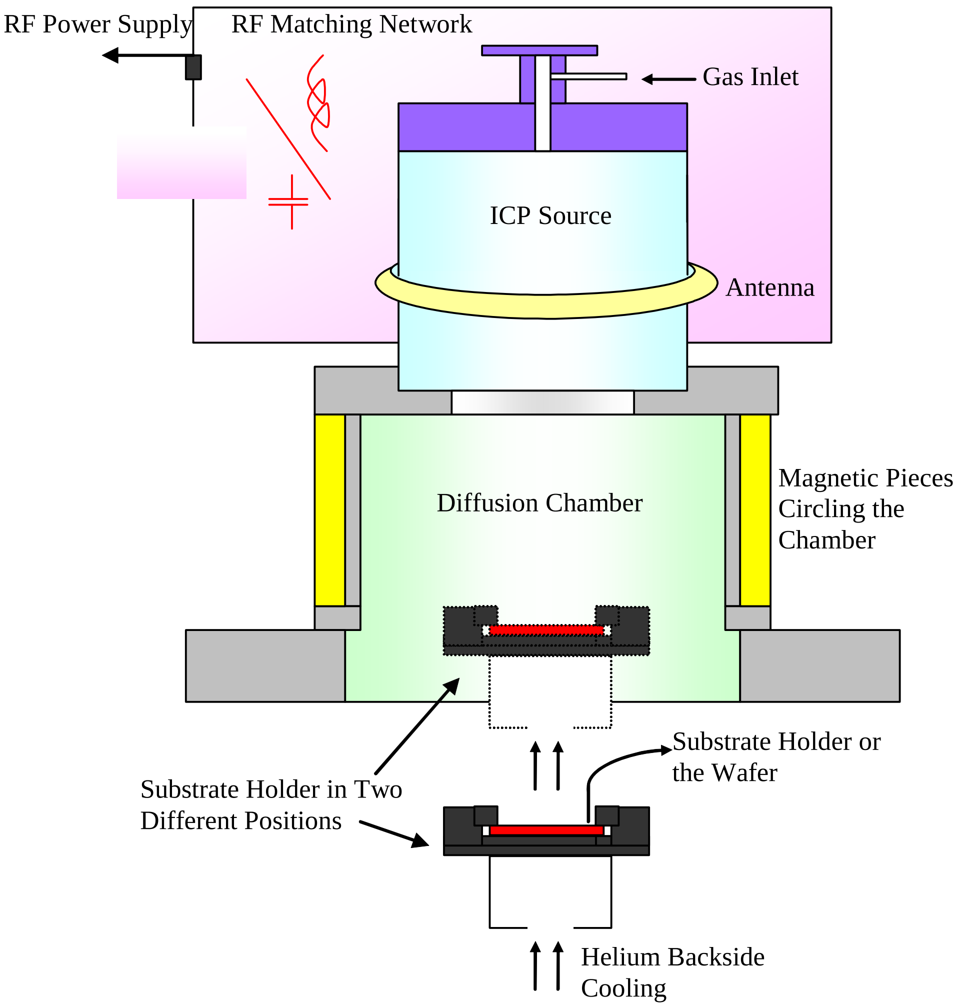

- Chamber lined with magnetic pieces.
- The temperature of the substrate was controlled using back side He cooling and a dedicated chiller.
- The ICP power is decoupled from the substrate power.
- The position of the substrate holder with respect to the ICP source could be varied.
- The RF power supplied operated at 13.56 MHz.

Sample Preparation

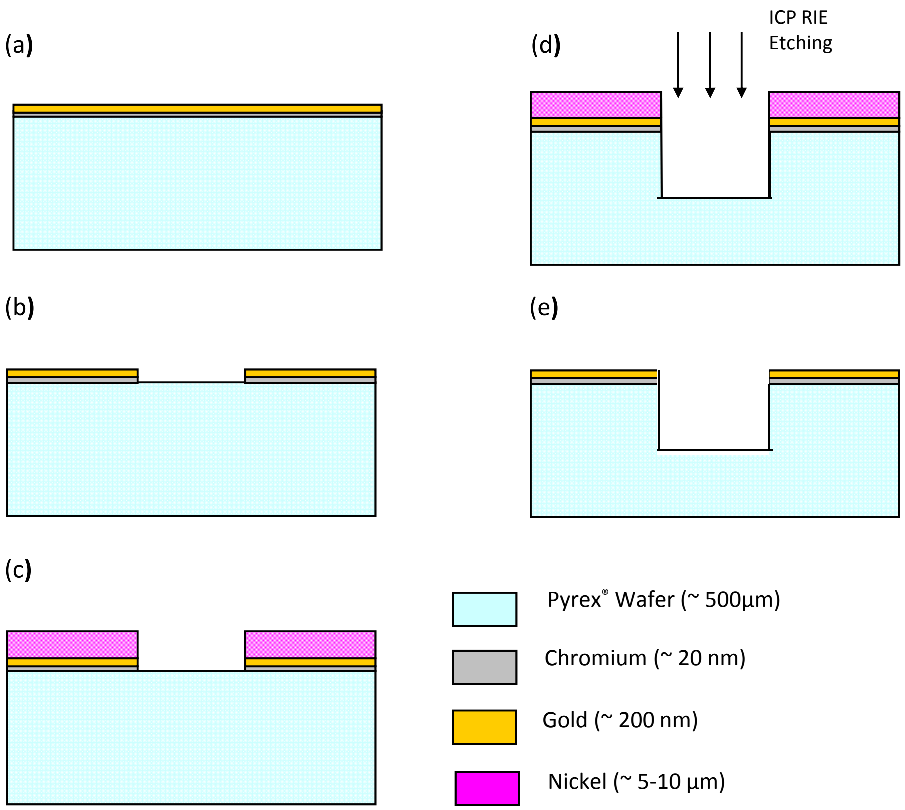

a) Deposition of Thin Layer of Au/Cr on top of Pyrex® 7740 wafer.
b) Patterning Au/Cr layer using standard lithography and etching steps.
c) Electroplating a thick (8-10 microns) layer of Nickel on the patterned seed layer.
d) ICP RIE etching step with electroplated Ni acting as a hard mask.
e) Removal of Nickel in a Piranha Clean solution.

Process Parameters

Process Design Parameter	Units of measurement	Experimental Range
ICP Power	Watts	500-2000
Substrate Power	Watts	100-475
O_2 Flow Rate	sccm	5-100
SF_6 Flow Rate	sccm	5-50
C_4F_8 Flow Rate	sccm	5-50
CH_4 Flow Rate	sccm	5-50
Ar Flow Rate	sccm	5-50
Operating Pressure	mTorr	1-20
Temperature of Substrate Holder	°C	5-30
Distance of Substrate Holder from ICP	mm	120-200

Design of Experiment Results

Nominal Etching Condition for SF_6/Ar chemistry

Process Parameter	Value	Units
ICP Power	2000	Watts
Substrate Power	475	Watts
Ar Flow Rate	50	sccm
SF_6 Flow Rate	5	sccm
Operating Pressure	< 2	mTorr
Distance From Source	120	mm
Substrate Holder Temperature	20	°C

Nominal Etching Conditions for the C_4F_8/SF_6/Ar/O_2 based chemistry

Process Design Parameter	Units of measurement	Optimum Value
ICP Power	Watts	2000
Substrate Power	Watts	475
O_2 Flow Rate	sccm	50
SF_6 Flow Rate	sccm	5
C_4F_8 Flow Rate	sccm	5
CH_4 Flow Rate	sccm	Not used
Ar Flow Rate	sccm	50
Operating Pressure	mTorr	Minimum possible
Temperature of Substrate Holder	°C	20
Distance of Substrate Holder from ICP	mm	120

Effect of Operating Pressure

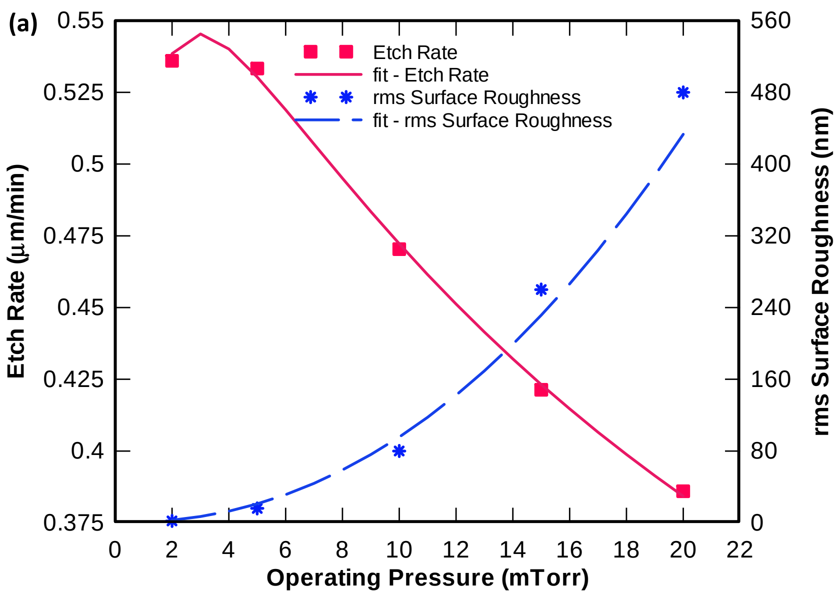

SF_6/Ar based chemistry

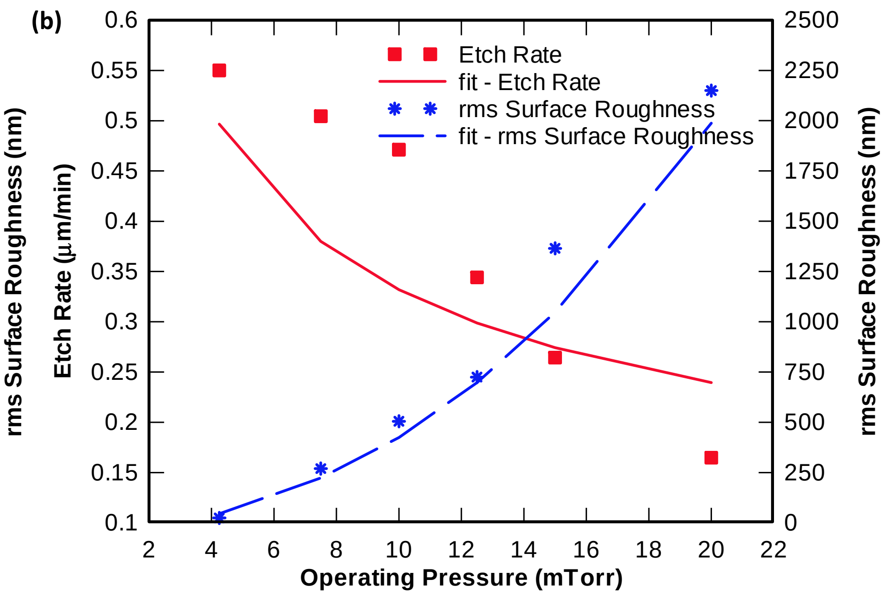

$SF_6/C_4F_8/Ar/O_2$ based Chemistry

Effect of ICP Power

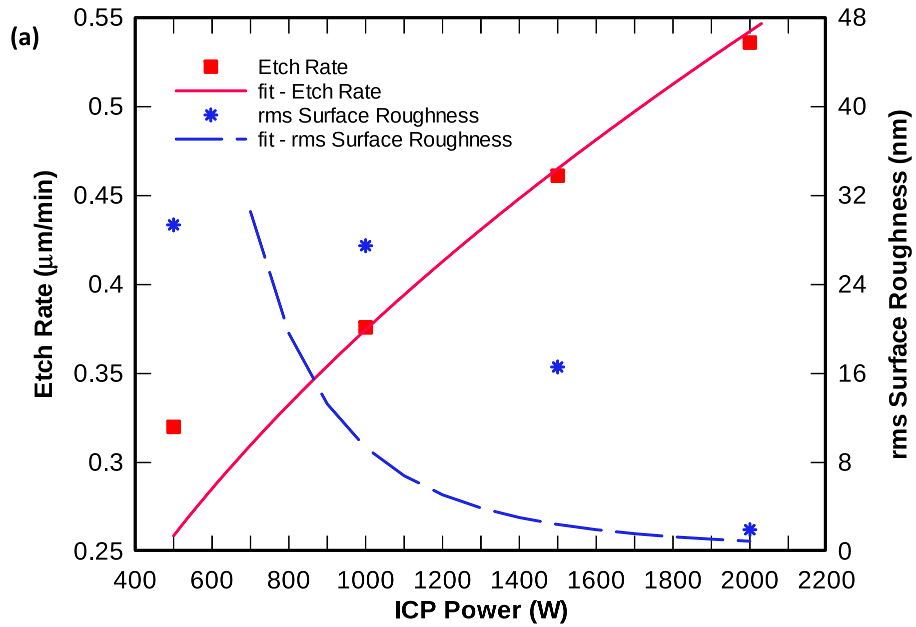

SF$_6$/Ar based chemistry

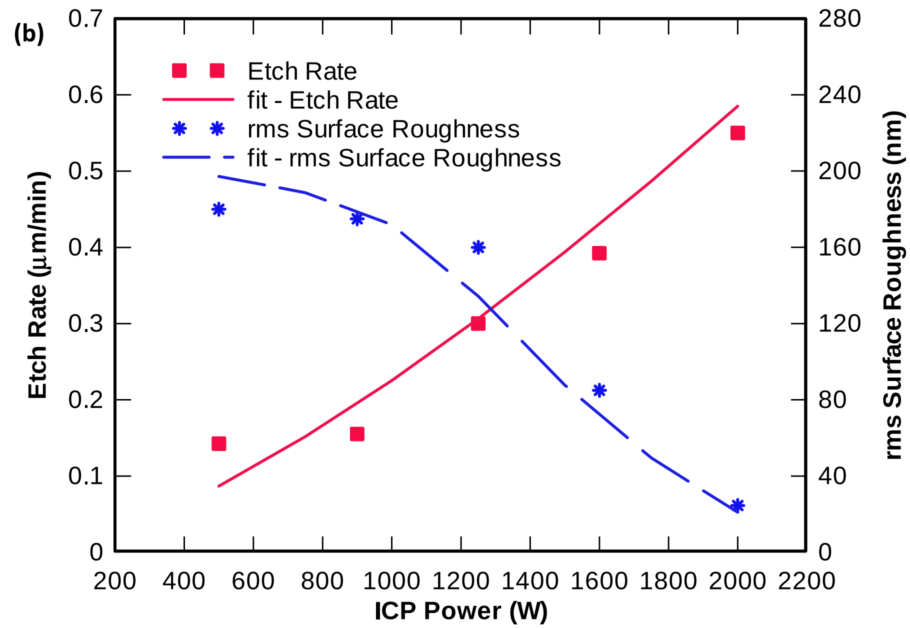

SF$_6$/C$_4$F$_8$/Ar/O$_2$ based Chemistry

Effect of Substrate Power

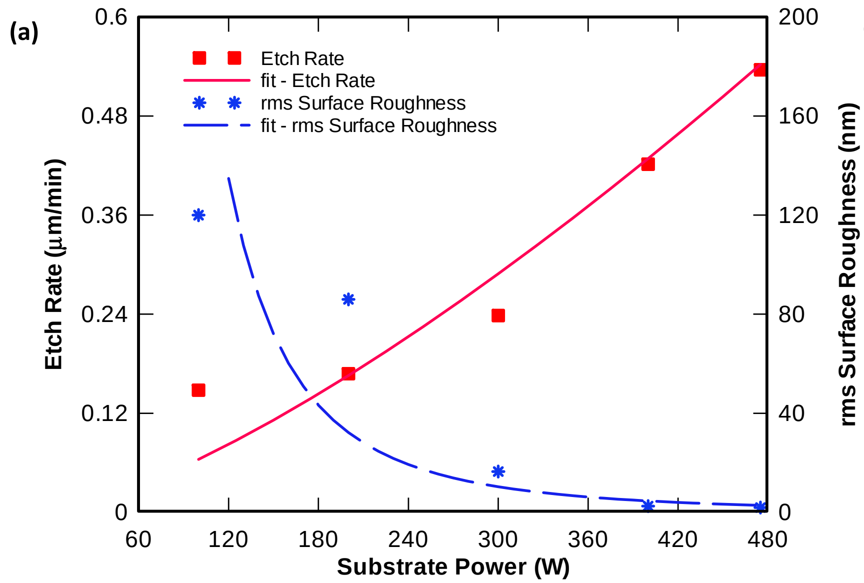

SF$_6$/Ar based chemistry

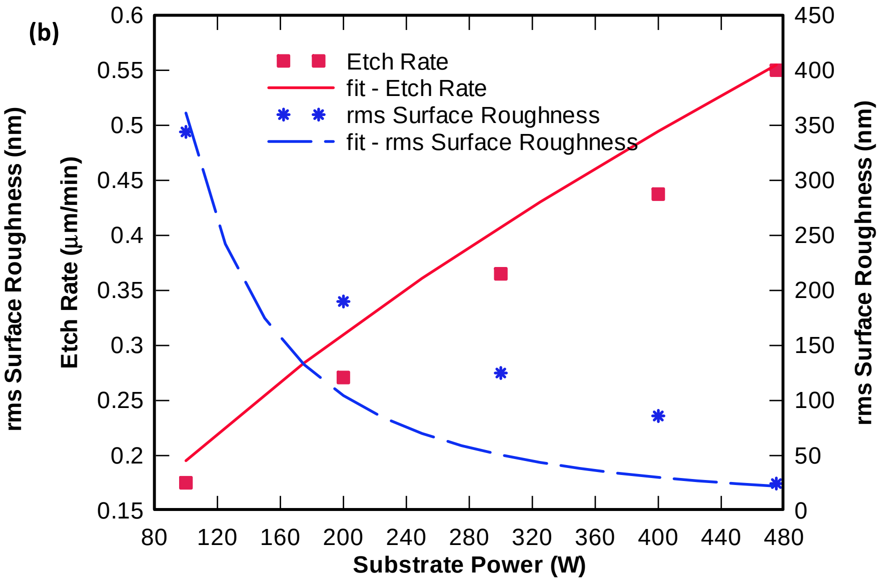

SF$_6$/C$_4$F$_8$/Ar/O$_2$ based Chemistry

Effect of Flow Rate of Gases

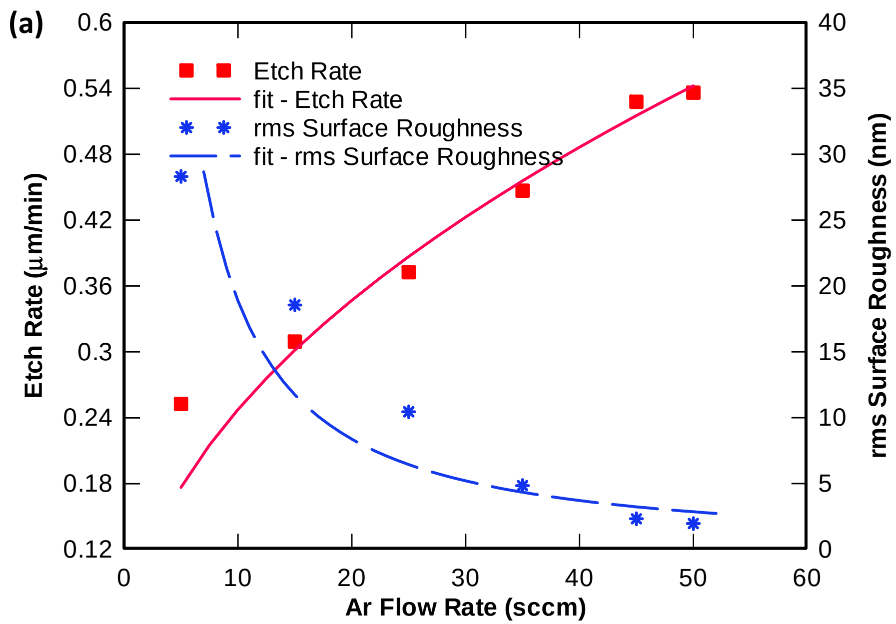

SF_6/Ar based chemistry

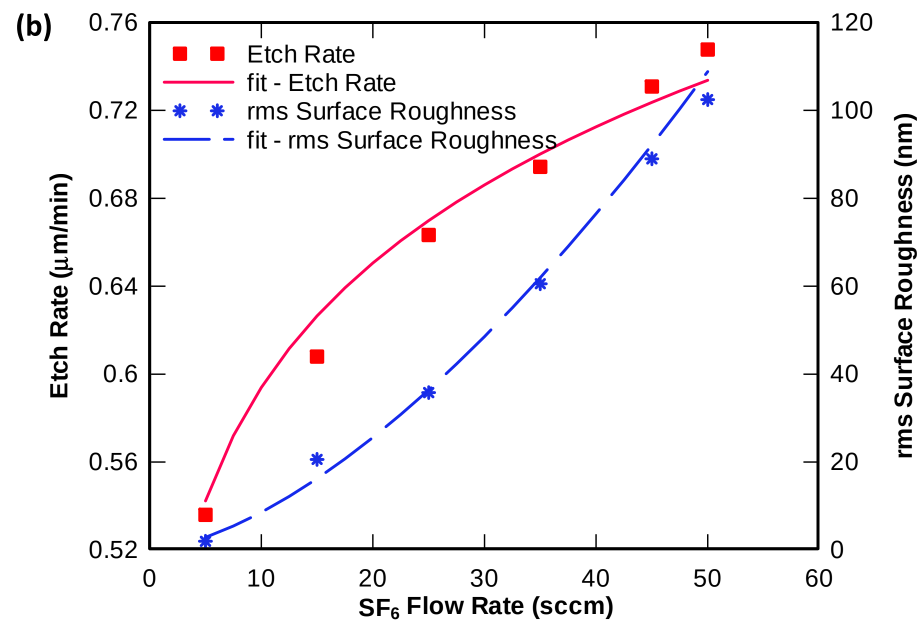

$SF_6/C_4F_8/Ar/O_2$ based Chemistry

Effect of Flow rate of Gases

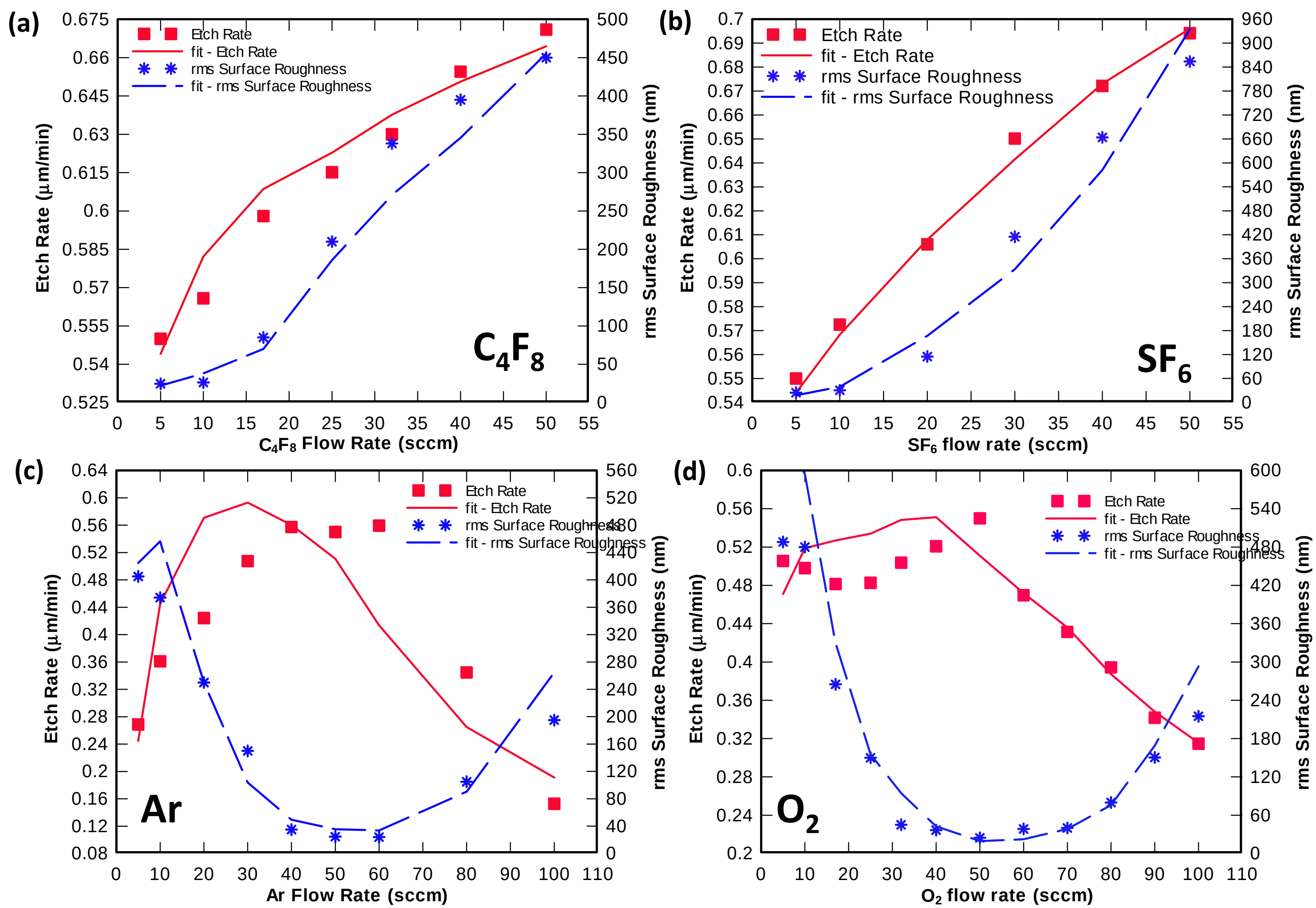

PENNSTATE MEMS

Effect of Distance from Source

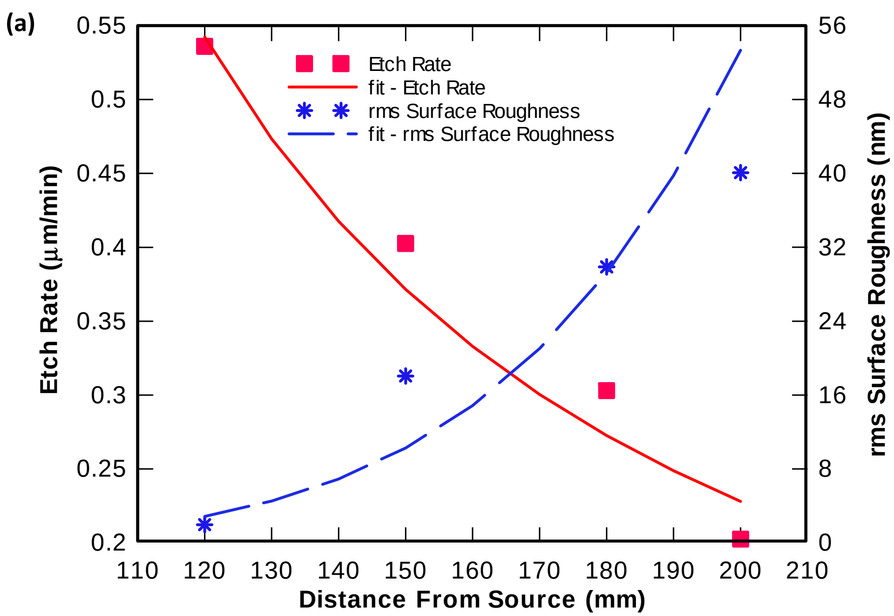

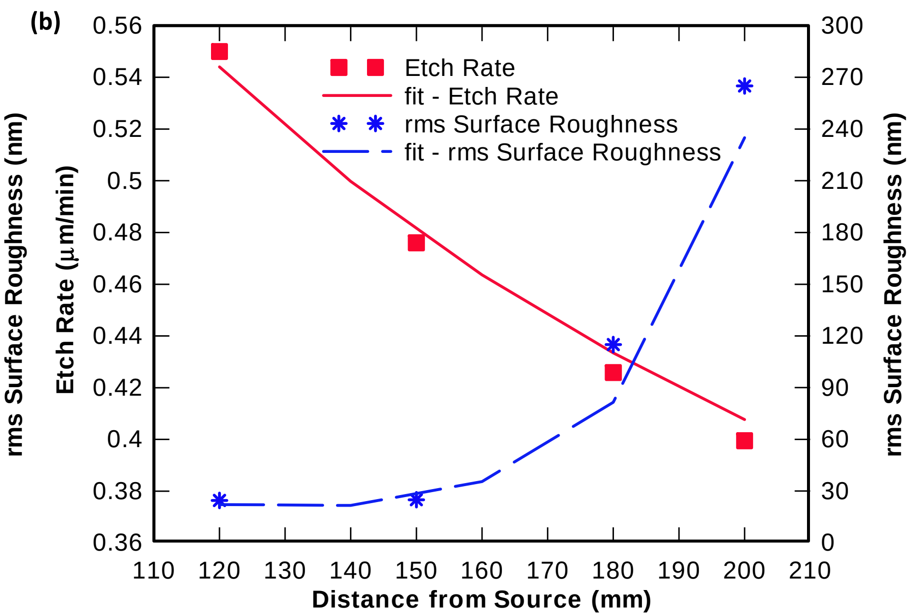

SF_6/Ar based chemistry

$SF_6/C_4F_8/Ar/O_2$ based Chemistry

Effect of Temperature

Temperature (°C)	SF_6/Ar chemistry		$SF_6/C_4F_8/Ar/O_2$ chemistry	
	Etch Rate (mm/min)	Rms Roughness (nm)	Etch Rate (mm/min)	RMS Roughness (nm)
5	0.498	2.1	0.5275	80
10	0.5	2	0.53	50
20	0.536	1.97	0.55	24.6
30	0.554	1.95	0.566	19.7

PENNSTATE MEMS

Surface Profile after Etching

After etching to a depth of 75 microns

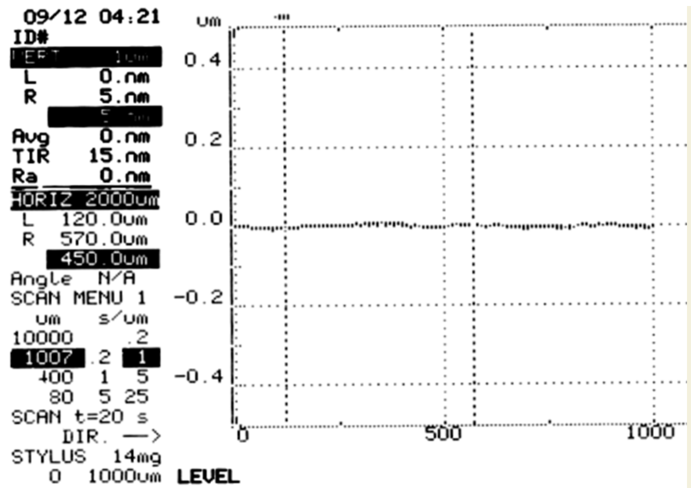

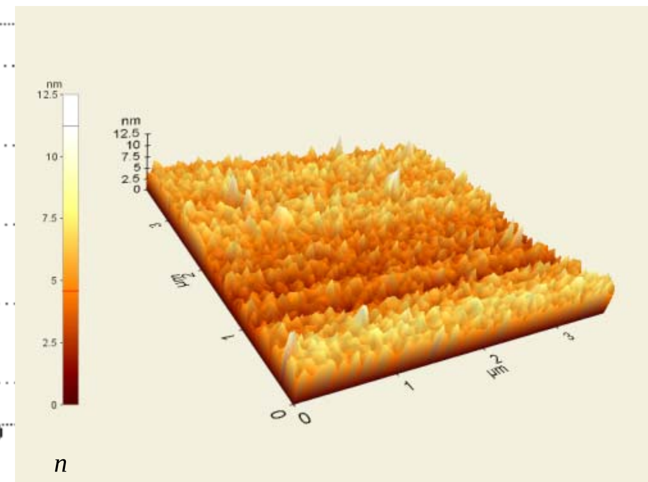

Statistics

Region	Min(nm)	Max(nm)	Mid(nm)	Mean(nm)	Rpv(nm)	Rq(nm)	Ra(nm)
Red	0.000	12.510	6.255	4.704	12.510	1.467	1.165

Typical Etch Profiles

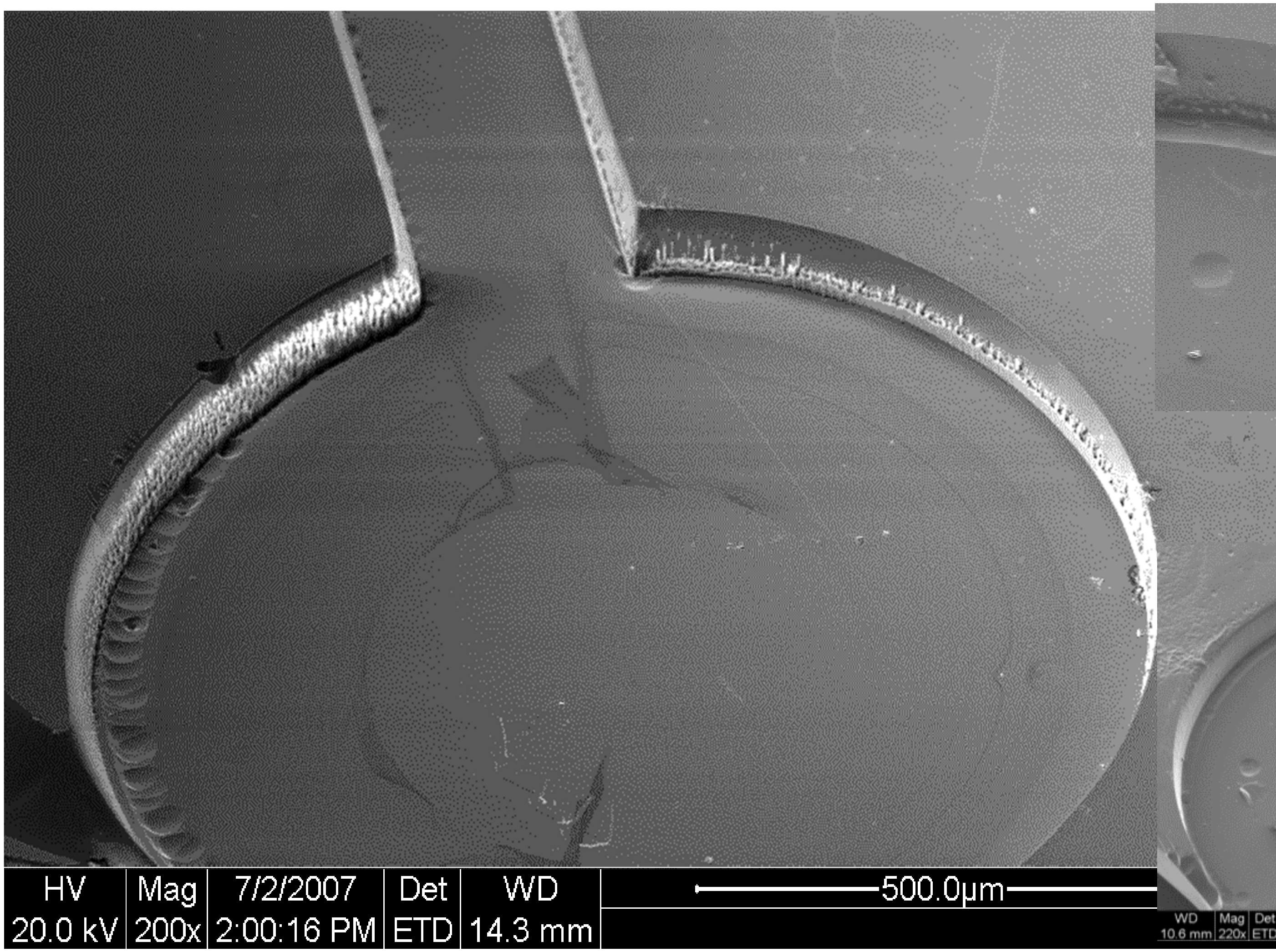

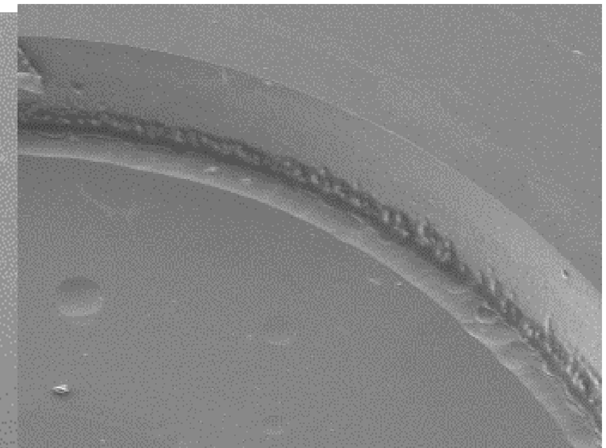

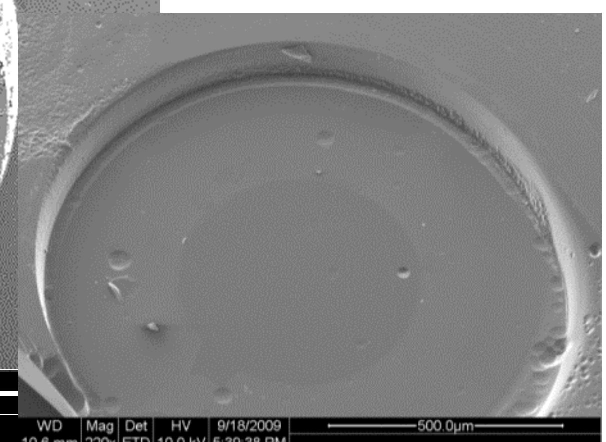

Quantization of the Etch Process

- Very useful to define a quantitative metric to relate process parameters to etch characteristics.
- Etch characteristics which vary monotonically with the process parameters can be modeled as power law.
- However, for etch characteristics which do not vary monotonically, higher order terms are required in the quantization process.
- We arranged the data in a m by (n+1) matrix, where m are the number of runs and n is the number of process parameters being quantized. The last column is the etch characteristic being quantized.

Quantization cont ….

- We then used a commercial software to fit the equation in the form to the data matrix

$$\ln(W) = \ln(a_0) + \sum_{i=1}^{n} a_i \ln(PP_i) + \sum_{k=2}^{3} \sum_{j=1}^{n} a_j \ln(PP_j^k)$$

where, W is the arbitrary number relating etch characteristics to the process parameters, a_i and a_j are the fitting parameters, PP_j are the process parameters whose effect on the etch characteristics are being quantized. Rewriting the equation by taking exponentials on both sides –

$$W = a_0 \left(\prod_{i=1}^{n} PP_i^{a_i}\right) \exp\left[\sum_{k=2}^{3} \sum_{j=1}^{n} a_j \ln(PP_j^k)\right]$$

For SF_6/Ar based Chemistry

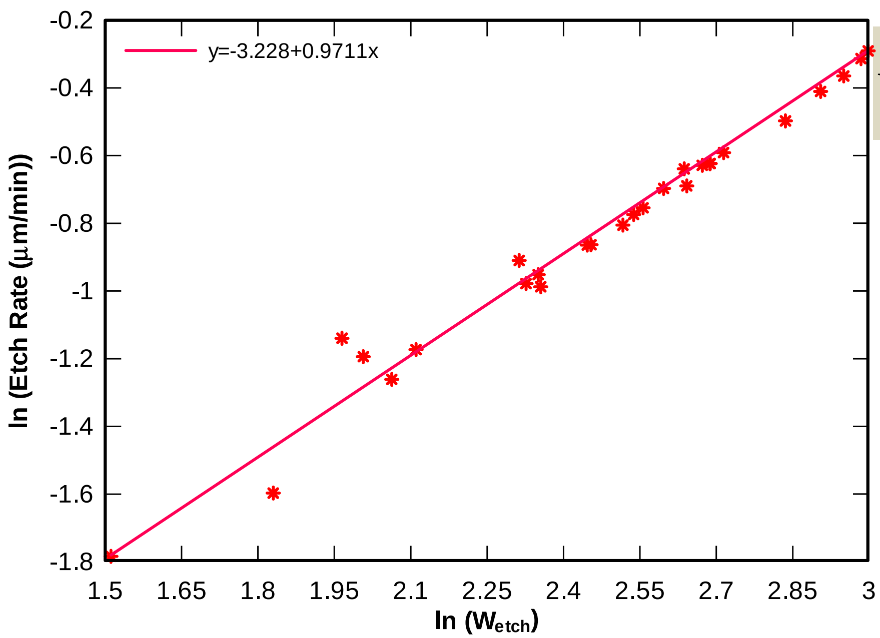

$$W_{etch} = \frac{W_{ICP}^{0.52} W_{sub}^{1.36} Q_{SF_6}^{0.135} Q_{Ar}^{0.48} T_{sub}^{0.065} P_{process}^{0.2}}{D^{1.67}} \exp(-0.094(\ln P_{process})^2)$$

$$\boxed{R_{etch} = aW_{etch}}$$

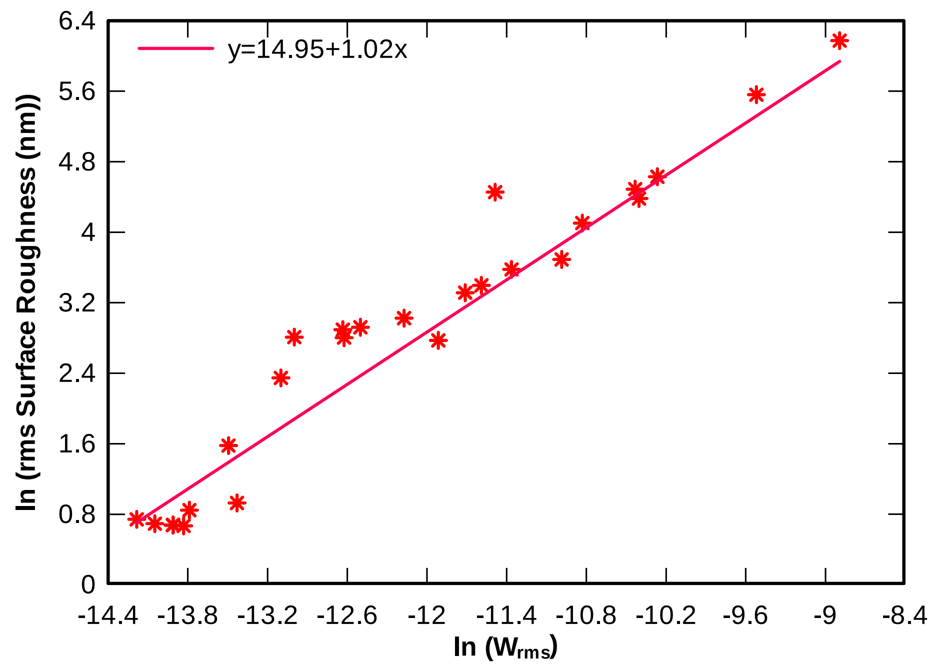

$$W_{rough} = \frac{Q_{SF_6}^{1.58} P_{process}^{2.18} D^{5.726} T_{sub}^{0.197}}{W_{ICP}^{3.173} W_{sub}^{2.8} Q_{Ar}^{1.172}}$$

$$\boxed{R_{rough} = bW_{rough}}$$

For $C_4F_8/SF_6/Ar/O_2$ based Chemistry

$$W_{etch} = \frac{W_{icp}^{1.38} W_{sub}^{0.68} Q_{Ar}^{2.78} Q_{O_2}^{1.32} Q_{C_4F_8}^{0.19} Q_{SF_6}^{0.23} T_{sub}^{0.000424}}{D^{0.465} P^{0.47}} \exp\{corr_1\}$$

$$\boxed{R_{etch} = cW_{etch}}$$

$$corr_1 = -0.42(\ln Q_{Ar})^2 - 0.18(\ln Q_{O_2})^2$$

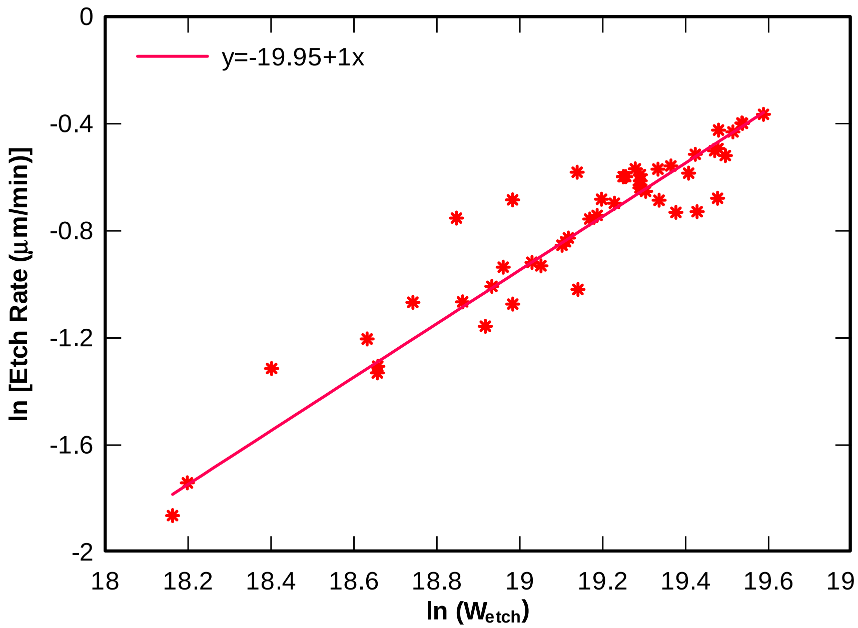

$$W_{rough} = \frac{W_{icp}^{66.39} Q_{Ar}^{30.13} Q_{C_4F_8}^{0.78} Q_{SF_6}^{0.83}}{W_{sub}^{1.79} Q_{O_2}^{50.5} D^{130.4} P^{2.23} T_{sub}^{0.67}} \exp\{corr_2\}$$

$$\boxed{R_{rough} = dW_{rough}}$$

$$corr_2 = -11(\ln Q_{Ar})^2 + 1.2(\ln Q_{Ar})^3 + 13.4(\ln D)^2 + 27.6(\ln Q_{O_2})^2$$
$$-6.8(\ln Q_{O_2})^3 + 0.6(\ln Q_{O_2})^4 + 0.2(\ln P)^2 - 0.04(\ln T)^2 - 4.8(\ln W_{icp})^2$$

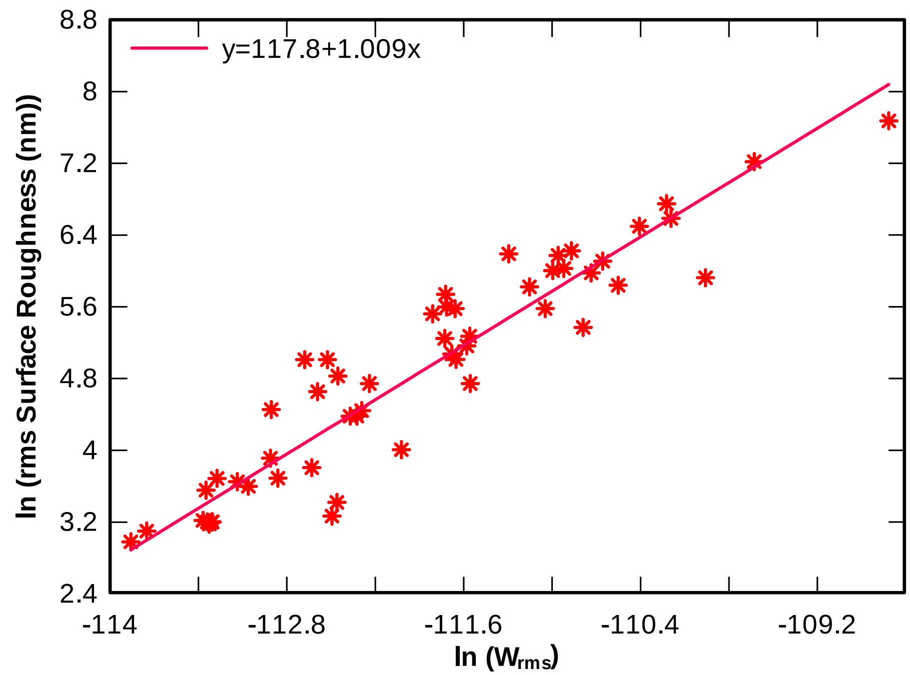

Etch Summary

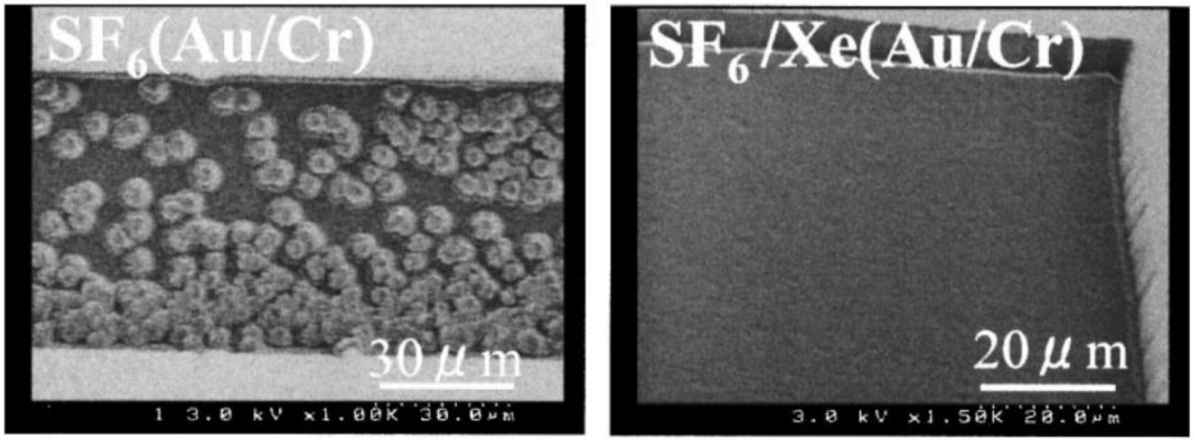

- Effect of removal of Cr/Au mask before etching
- Sidewall roughness and etch angle is primarily determined by the shape and quality of the mask sidewalls.
- Electroplating with resist pattern in place helps.

Li Li, Takashi Abe, Masayoshi Esashi, Smooth surface glass etching by deep reactive ion etching with SF_6 and Xe gases, J. Vac. Sci. Technol. B (2003) 21, 2545-2549.

NF_3 Based Etching

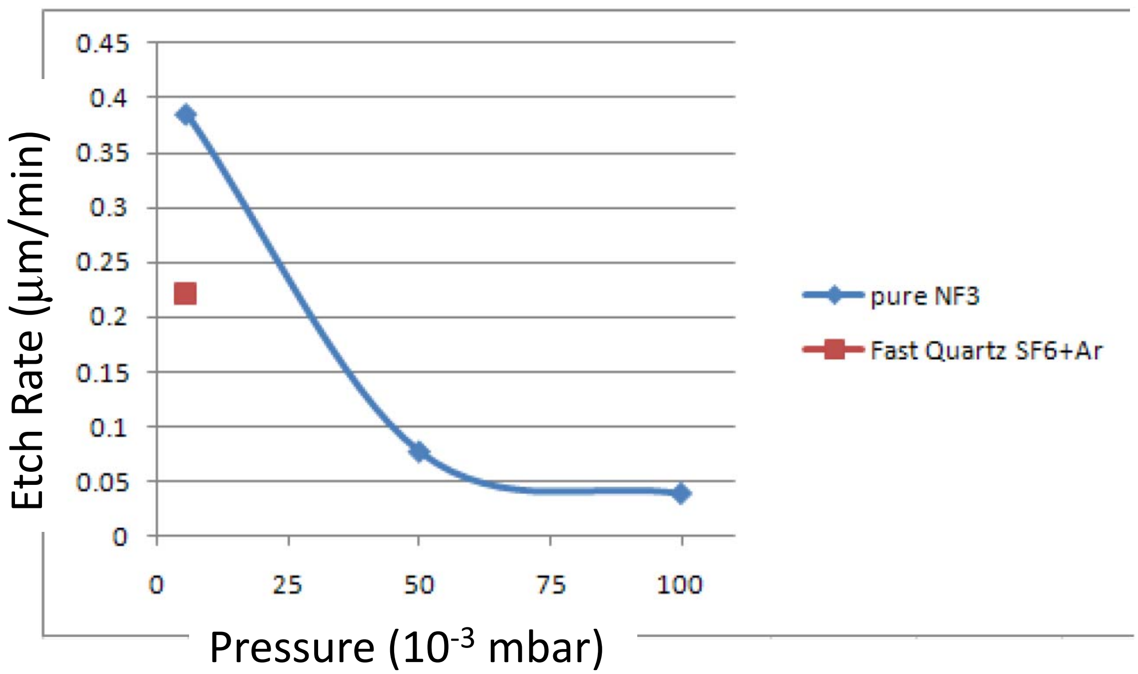

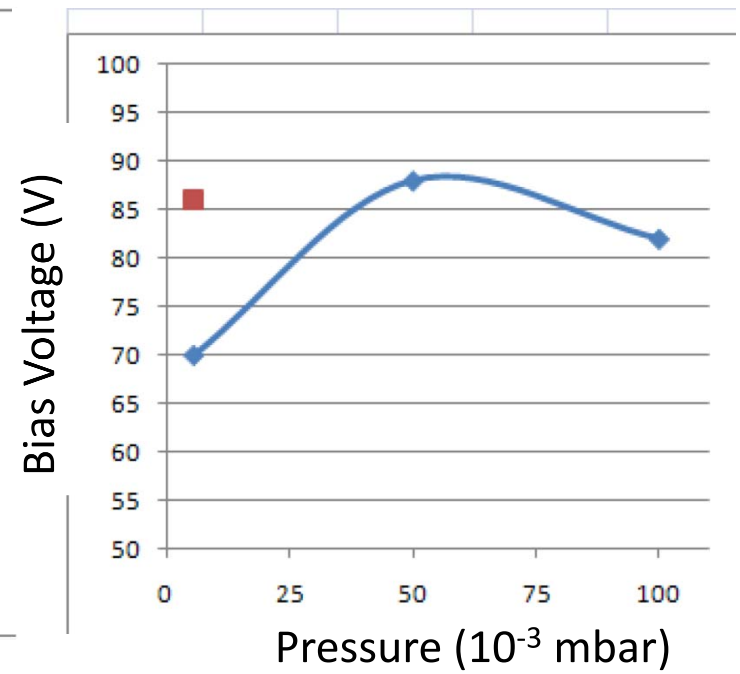

- NF_3 based etching shows better etch rate – also leads to a smaller etch bias for similar substrate and ICP power conditions

Etch Summary

– In ICP RIE process – low pressure improves etch rates since the kinetic energy of bombarding ions is higher due to the increased mean free path
– However, a trade off occurs since absolute number of ions/radicals impinging upon the etch surface decreases with pressure
– Fluorine improves the etch rate, but Ar is required to remove the non-volatile metal oxide residues.
– Thus an etch maximum in the 0.7 – 1.0 μm/min range has been observed.
– Furthermore increased energy leads to the use of hard mask such as nickel which is not ideal.
– Possible strategies exist including the exploration of organisilane gases, nitrohalogens etc.
– Non-equilibrium plasma processes have been seen to provide higher etch rates – however these require high pressures which is typically not possible in ICP-RIE systems

PENNSTATE MEMS

Overall Project Summary

The project was funded for $325,000 for a period of 4½ -years and has been very productive in terms of research output. The following accomplishments summarize the overall results from this project support:

- The first micromachined IR detectors from quartz crystal resonators were successfully demonstrated. Even in their first prototype versions, these detectors have shown performance that rivals some of the more established materials.
- Micromachined quartz resonators were used to evaluate the viscoelastic behavior of various globular proteins. Theses studies have shown how the self assembly process in protein layers leads to changes in their conformation and rearrangement of the layers. A comprehensive study on various surface types has been undertaken.
- Through a $25,000 supplement to the project, we have explored the use of nitrohalogen gas NF_3 for etching of glass and found a small enhancement in the overall etch rate of glass. However, a complete study of this could not be completed due to the short duration of the additional funding.
- **A total of 7 Peer Reviewed Journal Publications and 9 International Conference Presentations and 1 Patent were published by the funds supported by this grant.**
- One Ph.D. student graduated partly supported by the grant, one post-doctoral research associate was trained on this project, and one undergraduate student was involved in the project in addition to the principal investigator.